The other major finding of the review was that the less brain resection results in the less complication associated with CSF circulation [7]. We compared the rate of postoperative CSF shunt or Ommaya reservoir among periinsular hemispherotomy and transopercular hemispherotomy [4]. The latter was devised by Shimizu and Maehara to obtain larger working space in hemimegalencephaly by resecting frontotemporoparietal operculums. 9% of 11 procedures without opercular resection required postoperative CSF diversion while 47% of 15 procedures with opercular resection required it, suggesting that less brain resection resulted in the smaller occurrence of postoperative CSF circulation complications.

Our modification changed the anterior disconnection plane more posteriorly than the Delalande's original by connecting the anterior end of the choroidal fissure to the anterior end of the foramen of Monro, instead of the former to the subcallosal area. It is unknown that the small difference of resection volume really contributed to the decreased occurrence of CSF complication, and this must be confirmed in further studies. However, this minor modification may have a merit in completely disconnecting the residual epileptic tissues in cases with dysplasia in posterior orbitofrontal regions [9], and in reducing blood loss from perforating arteries of the anterior and middle cerebral arteries by avoiding cutting into the caudate nucleus. Of course, these speculations must be confirmed by further experience.

In our modified procedure we cut into the hypothalamus. We first worried about the risk of hypothalamic dysfunction, but we did not observe any disturbance in fluid and ion balance, body temperature, and others. Conventional anatomical hemispherectomy resects the significant amount of the hypothalamus but no severe hypothalamic dysfunction was reported. Therefore, we may not need to worry about this complication.

In conclusion, though these were minor modifications, they further minimized brain resection and may serve for less invasiveness of procedure and improvement in completeness of disconnection and its confirmation during surgery.

References

[1] Rasmussen T. Hemispherectomy for seizures revisited. Can J Neurol Sci 1983;10:71–8.
[2] Villemure JG et al. Hemispherectomy. In: Engel JJ, editor. Surgical Treatment of the Epilepsies. New York: Raven Press Ltd.; 1993. p. 511–8.
[3] Villemure JG, Mascott CR. Peri-insular hemispherotomy: surgical principles and anatomy. Neurosurgery 1995;37:975–81.
[4] Shimizu H, Maehara T. Modification of peri-insular hemispherotomy and surgical results. Neurosurgery 2000;47:367–72 Discussion 372–3.
[5] Schramm J, Kral T, Clusmann H. Transsylvian keyhole functional hemispherectomy. Neurosurgery 2001;49:891–900 Discussion 900–1.
[6] Delalande O et al. From hemispherectomy to hemispherotomy. In: Lüders HO, Comair YG, editors. Epilepsy Surgery. Philadelphia: Lippincott Williams & Wilkins; 2001. p. 741–6.
[7] Kawai K, Shimizu H. Clinical outcome and comparison of surgical procedures in hemispherotomy for children with malformation of cortical development. Epilepsia 2004;45(Suppl. 7):168.
[8] Kawai K et al. Clinical outcomes after corpus callosotomy in patients with bihemispheric malformations of cortical development. J Neurosurg 2004;101:7–15.
[9] Mittal S et al. Intractable epilepsy after a functional hemispherectomy: important lessons from an unusual case. Case report. J Neurosurg 2001;94:510–4.

Characteristic profiles of high gamma activity and blood oxygenation level-dependent responses in various language areas

Naoto Kunii, Kyousuke Kamada *, Takahiro Ota [1], Kensuke Kawai, Nobuhito Saito

Department of Neurosurgery, The University of Tokyo, 7-3-1 Hongo, Bunkyo-ku, Tokyo 113-8655, Japan

ARTICLE INFO

ABSTRACT

High gamma activity (HGA) has been shown to be positively correlated with blood oxygenation level-dependent (BOLD) responses in the primary cortices with simple tasks. It is, however, an open question whether the correlation is simply applied to the association areas related to higher cognitive functions. The aim of this study is to investigate quantitative correlation between HGA and BOLD and their spatial and temporal profiles during semantic processing. Thirteen patients with intractable epilepsy underwent fMRI and electrocorticography (ECoG) with a word interpretation task to evoke language-related responses. Percent signal change of BOLD was calculated at each site of ECoG electrode, which has power amplification of high gamma band (60–120 Hz) activity. We transformed locations of individual electrodes and brains to a universal coordination using SPM8 and made the quantitative comparisons on a template brain. HGAs were increased in several language-related areas such as the inferior frontal and middle temporal gyri and were positively correlated with BOLD responses. The most striking finding was different temporal dynamics of HGAs in the different brain regions. Whereas the frontal lobe showed longer-lasting HGA, the HGA-intensity on the temporal lobe quickly declined. The different temporal dynamics of HGA might explain why routine language-fMRI hardly detected BOLD in the temporal lobe. This study clarified different neural oscillation and BOLD response in various brain regions during semantic processing and will facilitate practical utilization of fMRI for evaluating higher-order cognitive functions not only in basic neuroscience, but also in clinical practice.

Introduction

A visualization technique of blood oxygenation level-dependent (BOLD) responses was developed as functional magnetic resonance imaging (fMRI) in the 1990s (Ogawa et al., 1990). Since then, fMRI has yielded a wealth of knowledge concerning various brain functions (Price, 2012). Meanwhile, it has been shown that fMRI activation includes a lot of subsidiary cortical areas unnecessary for actual implementation of a specific brain function. In particular, higher-order cognitive functions such as language seem to have wider supplementary areas, as several studies have shown that compared the fMRI results with electrocortical stimulation mapping (Bizzi et al., 2008; Kunii et al., 2011; Rutten et al., 2002). To utilize fMRI reliably in a clinical setting, we need to know in which situations the BOLD signal reflects the reality of neural activity. It is, therefore, of paramount importance to evaluate the concordance and dissociation between BOLD responses and underlying neuronal activity.

Power changes of oscillatory neuronal activities in various frequency ranges have recently received particular attention as physiological correlates of BOLD responses. Among them, the augmentation of high gamma activity (HGA) is assumed to reflect localized cortical processing and has been shown to be correlated with BOLD responses, mainly in the primary cortices such as the visual cortices of animals (Goense and Logothetis, 2008; Logothetis et al., 2001; Niessing et al., 2005) and the primary visual, auditory and motor cortices of humans (Hermes et al., 2011; Nir et al., 2007; Scheeringa et al., 2011). This assumption of HGA as a neural correlate of BOLD, that is, HGA–BOLD coupling, is supported by several basic studies as follows. Pharmacological (Hormuzdi et al., 2001; Traub et al., 2001), computer-simulation (Traub et al., 1997; Wang and Buzsaki, 1996) and electrophysiological studies (Cardin et al., 2009) suggested that HGA should be generated by synchronous post-synaptic potentials of fast-spiking GABAergic interneurons incorporated in a cortical assembly. On the other hand, approximately 74% of the energy budget of the brain was estimated to be devoted to post-synaptic potentials (Attwell and Iadecola, 2002). Taking these findings together, it is rational to assume that HGA could account for a large part of the blood oxygenation change.

---
* Corresponding author at: Department of Neurosurgery, Asahikawa Medical University, Asahikawa, Japan, 2-1, Midorigaoka-Higashi, Asahikawa, Hokkaido 078-8510, Japan. Fax: +81 166 68 2599.

E-mail address: kamady-k@umin.ac.jp (K. Kamada).

[1] Present address: Department of Neurosurgery, Tokyo Metropolitan Tama Medical Center, Tokyo, Japan, 2-8-29, Musashidai, Fuchu, Tokyo 183-8524, Japan.

On the other hand, there are a limited number of studies that investigated HGA–BOLD coupling in the association cortex. Lachaux et al. (2007) showed a close spatial correspondence of the coupling using depth electrodes in frontotemporal regions under semantic paradigms. Ojemann et al. (2009) undertook a detailed estimation of HGA–BOLD coupling in the temporal association cortex and found that HGA is a significant regressor of BOLD. Conner et al. (2011) studied the correlation between various frequency bands and BOLD in various cortices using subdural grids and found positive and negative correlations of BOLD with HGA and beta band oscillation, respectively. Although recent studies have gradually elucidated the relationships between brain oscillations and BOLD, detailed analysis of HGA–BOLD coupling in the human association cortices is needed for further progress of neuroimaging and neuroscience fields.

From previous language-fMRI studies, it is known that the temporal language areas are less activated by the various semantic paradigms than the frontal language areas (Kamada et al., 2007; Kunii et al., 2011; Rutten et al., 2002; Veltman et al., 2000). Kamada et al. revealed that fMRI had a higher sensitivity to the frontal language activity while magnetoencephalography to the temporal language activity. Rutten et al. explained that complex tasks such as sentence reading might activate the receptive language functions in the temporal lobe. Despite practical importance of reproducibility in imaging studies, it remains almost unknown why different imaging modalities and language tasks induce spatially different responses. It is important to clarify the fundamental difference between frontal and temporal language dynamics by analysis of HGA–BOLD coupling.

In this study, we focused on spatial and quantitative relationships of HGA–BOLD coupling in language areas. The results should contribute to providing supportive evidence of the robustness of fMRI. In order to elucidate the fundamental neurophysiology of language networks, regional differences between HGA dynamics and fMRI activation were investigated.

Materials and methods

Subjects

This study included 23 patients with intractable epilepsy who had undergone implantation of subdural electrodes for diagnostic purposes at the University of Tokyo Hospital since December 2006. Nine patients were excluded because they had a low intelligence quotient (<70) or no chance of preoperative fMRI evaluation. All the patients underwent the Wada test to investigate language lateralization. One patient, who had bilateral language representation as determined by the Wada test, was excluded from further studies. As a result, we investigated 13 patients (5 men, 8 women) with left language dominance. Detailed demographic data are shown in Table 1.

Table 1
Patient demographic and clinical characteristics.

Patient no.	Age (years), sex	Etiology	VIQ	Epileptic focus
1	36, Male	Cortical dysplasia	82	Right frontal
2	50, Female	Cavernous malformation	91	Right temporal
3	40, Male	Unknown	85	Left temporal
4	33, Female	Cortical dysplasia	94	Left frontal
5	40, Male	Unknown	93	Right temporal
6	26, Female	Unknown	87	Right temporal
7	47, Female	Cortical dysplasia	88	Right temporal
8	24, Male	Cortical dysplasia	83	Left temporal
9	35, Female	Arachnoid cyst	107	Left temporal
10	21, Male	Middle fossa encephalocele	79	Left temporal
11	36, Female	Unknown	72	Left temporal
12	36, Female	Mesial temporal sclerosis	97	Left temporal
13	22, Female	Unknown	79	Right temporal

VIQ = verbal intelligence quotient.

This study was approved by the research ethics committee of the faculty of medicine, University of Tokyo (approval number 1797). Written informed consent was obtained from each patient or their family before they participated in the study.

Language-fMRI data acquisition

In all patients, fMRI was performed more than two months before electrode implantation. MR imaging was performed using a 3-tesla MR scanner with echo planar capabilities and a whole-head receive-only coil (Signa, General Electric, USA). During the experiments, foam cushions were used to immobilize the patient's head. Before the fMRI session, three-dimensional T1-weighted MR images (3D-MRI) of the subject's brain were obtained, which consisted of 136 sequential, 1.4-mm-thick axial slices with a resolution of 256×256 pixels in an FOV of 240 mm. fMRI was performed with a T2*-weighted echo planar imaging sequence (echo time: 35 ms, repetition time: 4000 ms, flip angle: 90 degrees, slice thickness: 4 mm, slice gap: 1 mm, field of view (FOV): 280 mm, matrix: 64×64, number of slices: 22). Owing to the different head sizes and positions of each patient, we selected a large FOV that could always contain the entire head, fixing the same center of the FOV on the x- and y-axes for all sessions. This enabled simple and exact co-registration of the different image sessions.

Each fMRI session consisted of three dummy scan volumes, three activation periods, and 4 baseline (rest) periods. During each period, 5 echo planar imaging volumes were collected, yielding a total of 38 imaging volumes. To obtain language-fMRI data, we used a kind of reading task called the word interpretation task as follows.

Word interpretation task

Visual stimuli were presented on a liquid crystal display monitor, with a mirror above the head coil allowing the patient to see the stimuli. In the reading periods, words consisting of three Japanese letters were presented in a 2000 ms exposure time with interstimulus intervals of 500 ms. All letter strings were white with a black background. The patients were instructed to read the presented word silently and categorize it into "abstract" or "concrete" based on the nature of the word. During the rest periods, the patients passively viewed random dots of destructured letters that had the same luminance as the stimuli so as to eliminate primary visual responses. All words for the semantic tasks were selected from common Japanese words listed in the electronic dictionary produced by the National Institute for Japanese Language.

Language-fMRI data analysis

The functional imaging data were preprocessed and analyzed with SPM8 (Wellcome Department of Imaging Neuroscience, London, UK), implemented in MATLAB (The Mathworks, Inc., Natick, MA). The functional scans were realigned, normalized onto a template brain and spatially smoothed using a Gaussian filter (8 mm kernel). Preprocessed data of each patient were analyzed with the standard general linear model (GLM) approach using boxcar predictors convolved with the canonical hemodynamic response function (Friston et al., 1995). Low-frequency noise was removed with a high-pass filter (128 Hz). A second-level random effects analysis was performed on the contrast images generated for each individual to identify brain regions showing reliable differences between reading and rest periods. A P value of 0.005 uncorrected threshold was used to estimate the t-map. The resulting t-map was superimposed over a three-dimensional template brain using MRIcroN software (second-level fMRI map) (http://www.sph.sc.edu/comd/rorden/mricron/).

We utilized percent signal change of BOLD (BOLD-SC) to quantify the BOLD responses for each individual. A BOLD-SC is defined as the maximum height of the time course estimated for a task condition,

divided by the average signal across the whole session within a region of interest (ROI), and multiplied by 100. We defined a sphere-type ROI with 10 mm radius at the center of each electrode. The ROI analysis was performed using the Mars-Bar region of interest toolbox for SPM available on the Web at http://marsbar.sourceforge.net (Brett et al., 2002).

ECoG data acquisition

Each patient underwent electrode implantation for 2 to 3 weeks before resection of epileptogenic foci. We used grid and strip-type subdural electrodes, which consisted of silastic sheets embedded with platinum electrodes (3 mm in diameter), and a 10 mm interelectrode interval (center to center) (Unique Medical, Tokyo, Japan). Electrode locations were determined from post-implantation CT and aligned to pre-implantation volumetric MRI using EMSE v5.3 software (Source Signal Imaging, San Diego, CA). The estimated registration accuracy is ±2.5 mm, without accounting for surgical or MR imaging geometrical distortion (Ossadtchi et al., 2010).

ECoG recordings for this study were performed at least 48 hours after the last epileptic seizures. We confirmed also that the patients were not in epileptic states during and immediately after the recordings. Each patient was seated on a bed with a reclining backrest in an electrically shielded room. A computer monitor was placed 100 cm from the patient. Visual stimuli were presented using a Stimuli Output Sequencer (NoruPro Light Systems Inc., Tokyo, Japan). The resulting ECoG were digitally recorded at a sampling rate of 400 Hz, using a 128-channel EEG system (BMSI 6000, Nicolet Biomedical Inc., Wisconsin). The band-pass filter for the data acquisition was set to 0.55–150 Hz. Electric triggers generated by the stimulus computer were simultaneously recorded with one of the EEG channels. A reference electrode was placed on the scalp at Cz (international 10–20 system). The stimuli for the language task consisted of the same words used in the word interpretation task of the fMRI session. All letter strings were presented for 350 ms with randomly variable interstimulus intervals, ranging between 2700 and 3300 ms. The words were displayed randomly, and each was presented once or twice, yielding 100 data epochs. The patients were instructed to read the words covertly and categorize them into "abstract" or "concrete."

ECoG data processing

All analyses of the ECoG data were performed using custom software written in Matlab R2008b. We focused on the electrodes on the lateral surface of the dominant hemisphere, which showed language-related activations on fMRI. The baseline and reading periods for all analyses were −600 to −100 ms pre-stimulus and 0 to 750 ms post-stimulus, respectively. On the basis of a visual inspection of the ECoG signals, epochs involving singular noises and epileptic spikes were excluded from further analysis. Fast Fourier transformation was performed every 1 Hz using 250 ms windows with 125 ms step sizes to obtain power spectral density estimates. A Hanning window was imposed on each data window to attenuate edge effects (Fig. 1A).

To obtain the power average across the high gamma range, we standardized the power spectral density estimates with respect to the 1500 ms data epochs consisting of pre- and post-stimulus 750 ms data epochs (Fig. 1B). This flattened out the spectral landscape, which allowed averaging across frequencies (Leuthardt et al., 2007). We defined a high gamma power change (HG-PC) as a standardized spectral power change from baseline to reading periods in a high-frequency band (60–120 Hz) (Fig. 1C). A t-test was performed to test whether the HG-PC was significantly larger than zero, and results were reported at $P < 0.05$, Bonferroni-corrected for the number
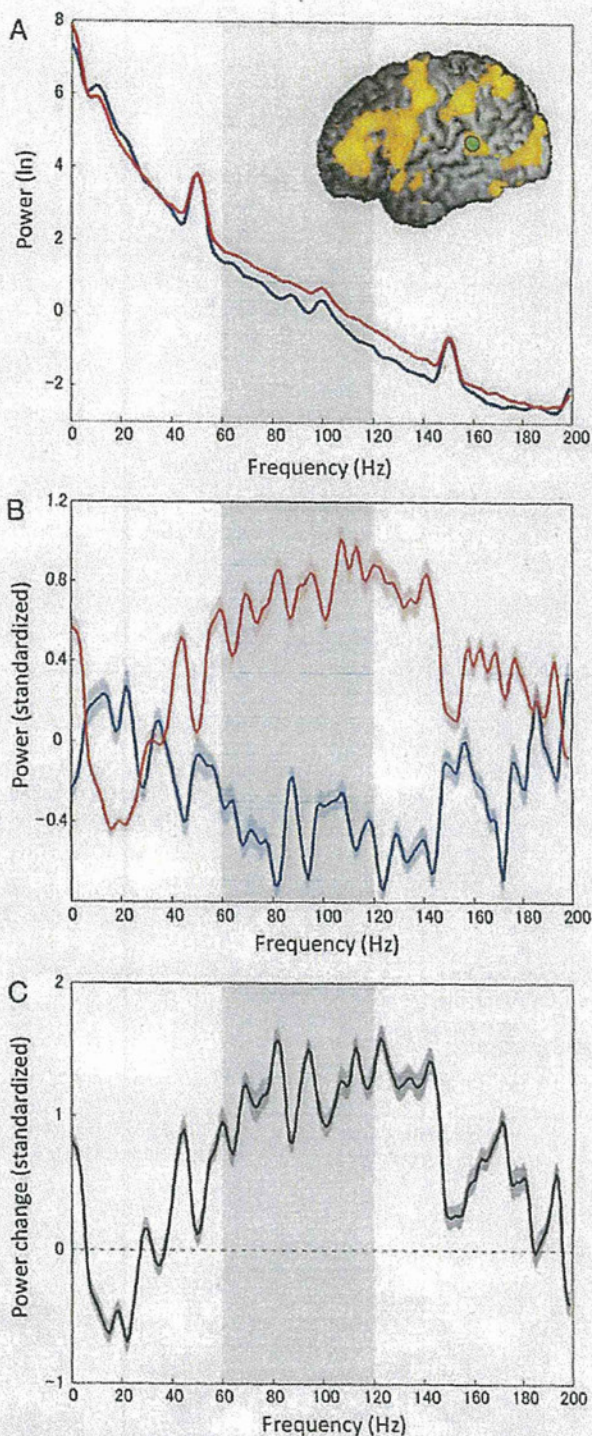

Fig. 1. Frequency profiles of an electrode (green dot on the left superior temporal gyrus). The light-gray zones indicate the high gamma frequency range (60–120 Hz). (A) Power spectral density functions in reading (red line) and rest (blue line) periods. The power was increased in the high gamma frequency range during the reading task. (B) Standardized power spectral density functions in reading and rest periods. Standardized power versus frequency was compared between the reading (red line) and rest periods (blue line). The shaded areas around the solid lines indicate standard errors of the mean values for each period. (C) Subtraction of the spectral density functions between reading and rest periods. The shaded area around the solid line indicates standard errors of the mean values.
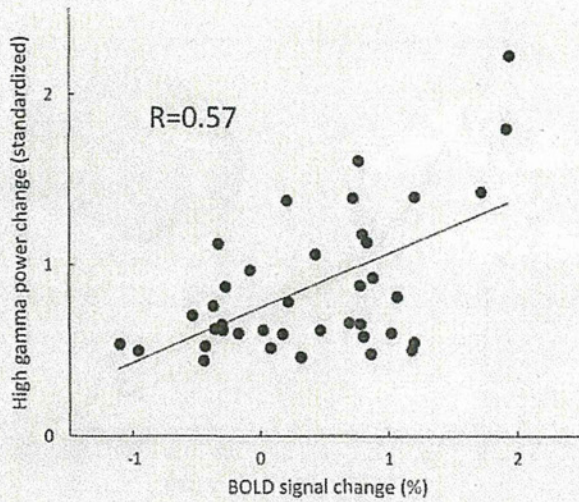
Fig. 2. Scatter plots of standardized high gamma power changes against BOLD signal changes. Regression analysis showed a positive correlation between them ($R = 0.57$, $P = 0.0002$).

of electrodes. The electrodes with significant or non-significant HG-PC are indicated as HGA(+) or HGA(−), respectively.

Statistical analysis

We tested whether BOLD responses correlated with HGAs. For each HGA(+) electrode, the BOLD-SC and HG-PC were calculated as described above. A linear regression model was fitted and tested for significance by an F-test.

For a better description of the relationship of HGA and BOLD in the frontal and temporal lobes, we made detailed comparisons across them: BOLD-SC responses between HGA(+) and HGA(−) sites, HG-PCs between the frontal and temporal lobes, and BOLD-SC between the frontal and temporal lobes, separately, according to the HGA profiles. To test the differences, we used Wilcoxon's rank sum test ($P < 0.05$).

Electrode normalization and visualization on a template brain

To elucidate whether HGA(+) electrodes were located predominantly in the primary areas (e.g. sensori-motor cortex), we spatially

normalized HGA(+) electrodes and displayed them on a template brain. A detailed procedure of electrode normalization is described elsewhere (Kunii et al., in press). This HGA distribution map was compared with the result of the second-level analysis of fMRI data.

Time-frequency analysis

To compare HGA dynamics in the frontal and temporal lobes, we further employed time-frequency analysis. The detailed procedure is described elsewhere (Kunii et al., in press). Briefly, we used spectrograms to estimate the energy density of the signals in the time-frequency plane. Short-time Fourier transformation was performed on the windowed epochs with 90% overlap. We performed a permutation test to determine P values for each time–frequency point of the spectrograms. The obtained P-value maps were corrected for multiple comparisons (false discovery rate correction, $P < 0.05$).

To quantify the high gamma activity in the time course, we counted the number of frequency bins that displayed significant activity at each time point within the range of 60–120 Hz. We termed the resultant number the high gamma broadband index (HGBI).

Results

Finally, we investigated 478 electrodes, which covered the lateral surface of the dominant hemisphere on a template brain (Fig. 3A), and found 39 electrodes were HGA(+) (Fig. 3B). The mean values of BOLD-SC at HGA(+) and HGA(−) sites were 0.39 and 0.21, respectively, without a significant difference between them.

The regression analysis showed moderate correlation between HG-PC and BOLD-SC at HGA(+) sites ($R = 0.57$, $P = 0.0002$) (Fig. 2).

HGA(+) electrodes were localized in the inferior frontal, superior and middle temporal, and precentral gyri (premotor cortex and face-motor area) (Fig. 3B). A second-level fMRI map was displayed on the template brain (Fig. 3C). We compared distributions between BOLD activities and HGA(+) sites by visual inspection. In the frontal lobe, the distributions of the two activities generally matched. In the temporal lobe, however, considerable mismatch was observed, particularly in the superior temporal gyrus. HGAs were frequently localized in the superior temporal gyrus, whereas significant BOLD activities were not. Instead, wide BOLD activities appeared in the posterior inferior temporal gyrus, where ECoG electrodes were scarcely placed.

In order to explain the HGA–BOLD mismatch between the frontal and temporal lobes, we investigated the HGA profiles and found no significant difference of HG-PCs (Fig. 4B). In addition, there was no significant difference of frequency distribution in HGA on each lobe
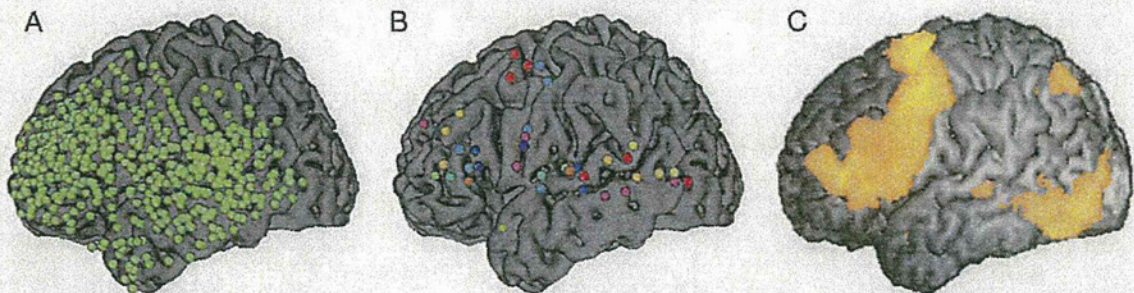

Fig. 3. Comparisons between distributions of high gamma activities (HGAs) and BOLD responses on a template brain. (A). All ECoG electrodes displayed on a template brain. The electrodes (green dots) on the template brain widely covered the lateral aspect of the left frontal and temporal lobes. (B) ECoG electrodes with significant HGA. Different colors of the electrodes indicate individual patients. The electrodes were mainly clustered on the inferior frontal, superior and middle temporal, and precentral gyri (premotor cortex and face-motor area). (C) A three-dimensional t-map of across-individual BOLD response displayed on a template brain. The BOLD responses were widely observed in the frontal lobe, which involves the inferior frontal and precentral gyri. There were additional activated areas in the inferior temporal gyrus, which were sparsely covered by ECoG electrodes.
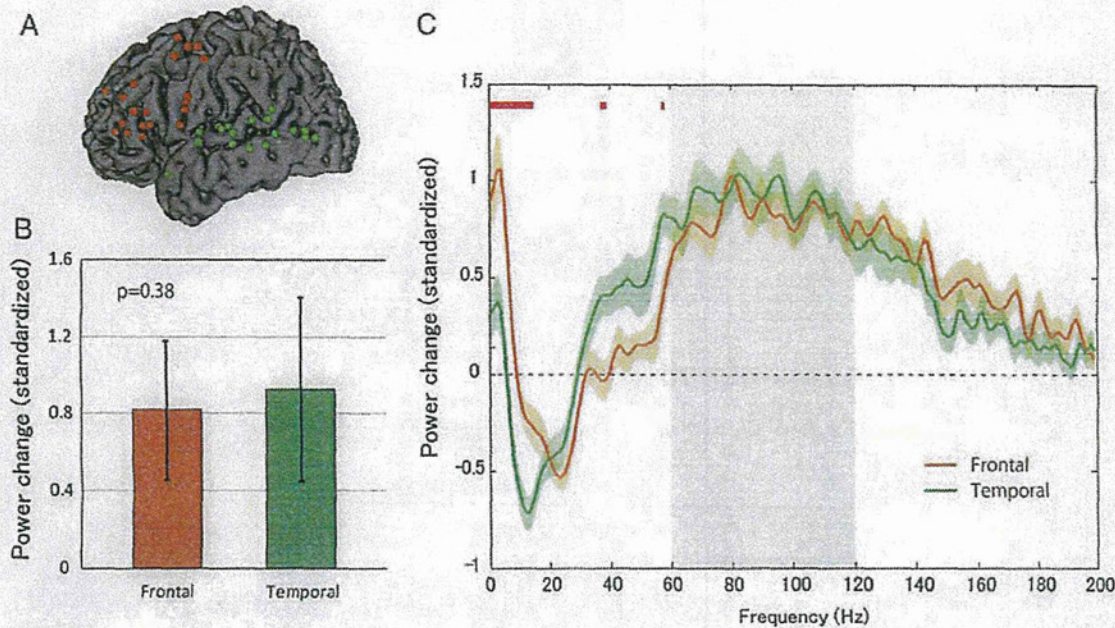
Fig. 4. Comparison of high gamma activity (HGA) between the frontal and temporal lobes. (A) Frontal (orange) and temporal (green) electrodes with significant HGAs. (B) Standardized power changes at the frontal (orange) and temporal (green) electrodes. There was no significant difference of high gamma activity between the frontal and temporal lobes. The error bars indicate the standard error of the mean and the P-value is based on Wilcoxon's rank sum test. (C) Spectral density functions of the standardized power changes in the frontal (orange) and temporal (green) lobes. Orange and green lines indicate the grand averages of spectral density functions in the frontal and temporal lobes, respectively. Red bars above the lines indicate significant differences of spectral density functions between frontal and temporal lobes (P<0.05). Power increase in the theta range and decrease in the alpha range were stronger in the frontal and temporal lobes, respectively. There was no significant difference in the high gamma frequency range. The shaded area around the solid line indicates standard errors of the mean values. A light-gray zone indicates the high gamma frequency range (60–120 Hz).

(Fig. 4C). Note that we observed differences in other frequency ranges. Increased oscillatory activity in the theta range compared to the baseline (theta synchronization) was stronger in the frontal than the temporal lobe and decrease in the alpha range (alpha desynchronization) was dominantly observed in the temporal lobe.

We investigated whether the existence of HGA could affect the BOLD activities in the frontal and temporal lobes (Fig. 5). In HGA(+) sites, there was no significant difference between BOLD-SCs in the frontal and temporal lobes. In HGA(−) sites, on the other hand, BOLD-SCs were significantly higher in the frontal than in the temporal lobe (P = 0.038).

We then focused on temporal profiles of HGA in each lobe using time-frequency analyses. We investigated several brain regions such as the inferior frontal, precentral (premotor cortex and face motor area), middle and posterior superior temporal, and posterior middle temporal gyri, where the HGA(+) electrodes were clustered (Fig. 6). Each cluster showed characteristic temporal changes of HGA. In particular, the HGBI time courses of the temporal lobe had short latencies and declined rapidly at 500 ms with short duration. On the other hand, those of the frontal lobe had later onset with longer duration. Each lobe had independent and characteristic HGA dynamics.

Discussion

We observed language-related HGA and BOLD derived from 13 patients with intractable epilepsy and made detailed comparisons between them on a template brain. HGAs appeared not only in the primary motor area, but also in the language-related association cortices. Each region contained two or more HGA(+) electrodes, suggesting

these areas showed the augmentation of HGAs consistently. In these HGA(+) regions, we demonstrated a positive correlation between HGAs and BOLD responses, and electrical oscillation could be a
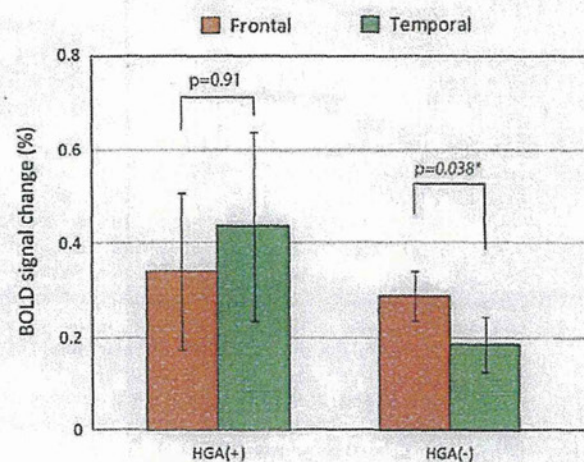

Fig. 5. Comparison of BOLD responses between the frontal (orange) and temporal (green) lobes. BOLD signal changes in each lobe were compared depending on high gamma activity (HGA) profiles (positive or negative). The BOLD responses with negative HGA were significantly higher in the frontal lobe than in the temporal lobe. There was no significant difference in the BOLD responses with positive HGA between the two lobes. The error bars indicate the standard error of the mean and the P-value is based on Wilcoxon's rank sum test.
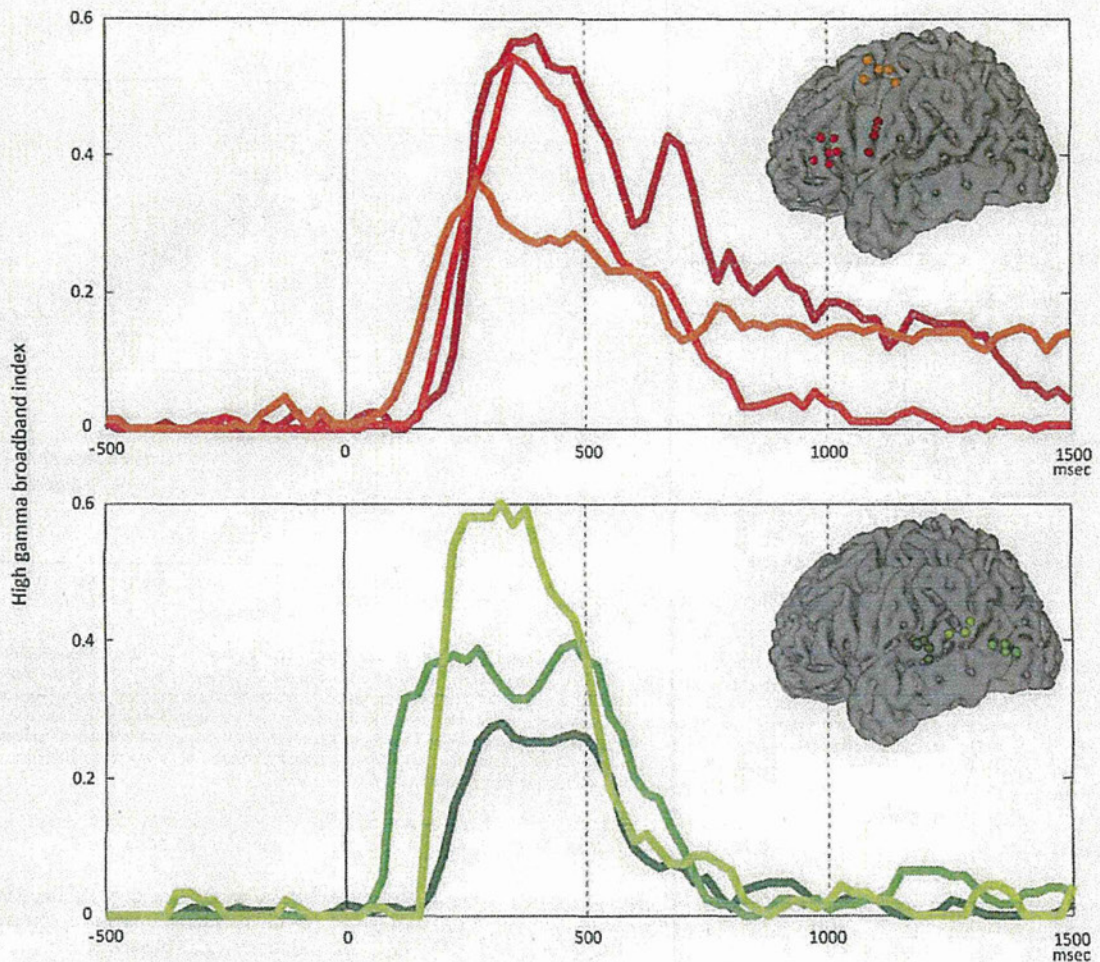
Fig. 6. Temporal dynamics of high gamma activity of noticeable electrode clusters in frontal and temporal lobes. Each line color corresponds to electrode color. X and Y axes indicate latency and high gamma broadband index (HGBI), respectively. HGBI in the frontal lobe lasted longer beyond 1000 ms. On the other hand, rapid decline of HGBI was observed after 500 ms in the temporal lobe.

physiological counterpart of BOLD signals. In addition, we found BOLD-HGA spatial mismatch and differences of HGA dynamics in the frontal and temporal lobes.

Previous studies have reported that the local field potentials (LFPs) positively correlated with BOLD responses in the primary cortices (e.g., visual, sensory, motor) of animals and humans (Goense and Logothetis, 2008; Hermes et al., 2011; Logothetis et al., 2001; Niessing et al., 2005; Nir et al., 2007; Scheeringa et al., 2011). Such LFP-BOLD coupling is assumed to be a measurable counterpart of neurovascular coupling, which is of paramount importance in interpreting the results of fMRI in neuroimaging research and clinical situations. The aim of this study is to clarify the neurovascular coupling in the human association cortex (language-related) by analyzing neuronal oscillations represented by HGA. Although LFP-BOLD coupling in the primary cortical areas was robust, some researchers have raised concerns over dissociation between LFPs and BOLD signals in other cortical areas (Arne, 2010). In fact, we observed no significant difference of BOLD responses between HGA(+) and HGA(−) sites, meaning that there were considerable BOLD responses without HGAs in association cortices. This finding seemed to reflect a wider distribution of hemodynamic BOLD responses around the corresponding electrical activities, which might have caused difficulties in demonstrating HGA-BOLD coupling in association cortices. In this study, we showed that HGAs were

positively correlated with BOLD responses by including only BOLD responses at HGA(+) sites. We believe that our findings provide supportive evidence to elucidate HGA-BOLD coupling in association cortices.

The fMRI group analysis showed a spatial dissociation between BOLD responses and HGAs in the temporal lobe. Our study showed the reading task induced less BOLD responses in the temporal lobe, which was in line with the findings of previous studies (Kamada et al., 2007; Kunii et al., 2011; Rutten et al., 2002; Veltman et al., 2000). In order to determine the reasons for the spatial dissociation of HGA-BOLD coupling in the temporal lobe, we made detailed comparisons of HGA between the frontal and temporal lobes. The two lobes showed no significant difference of power spectral density in the high gamma band. Therefore, it might be hard to fully explain the dissociation of HGA and BOLD distribution between frontal and temporal lobes only by spectral characteristics of HGA. Interestingly, the BOLD responses in HGA(−) sites were significantly weaker in the temporal than in the frontal lobe. We speculated that BOLD responses in HGA(−) sites were more widely distributed around HGA(+) sites in the frontal than in the temporal lobe. In order to explain our hypothesis, we considered that the most important facts were HGA temporal profiles, assuming that prolonged electrical activation could evoke wider hemodynamic responses. According to the time-frequency analysis, the HGAs in the frontal lobe *tended to be*

longer-lasting than those in the temporal lobe. Such different temporal patterns of HGAs in each lobe might have generated the different BOLD responses around the functional epicenters, which could have led to the dissociation of the spatial distributions of HGAs and BOLD responses.

In this study, we used the word interpretation task, in which semantic decisions were needed after covert word reading. The inferior frontal lobe is strongly related with executive roles in semantic decisions (Badre and Wagner, 2007; Binder et al., 2009; Fiez, 1997; Martin et al., 1995, 1996; Noppeney et al., 2004; Thompson-Schill et al., 1997; Wagner et al., 2001). It seems that our task effectively induced HGA in the frontal association cortices, which might be the key for the excellent overall HGA–BOLD coupling. Wu et al., reported picture naming task elicited wider gamma oscillations in temporo-parietal regions than simple word reading (Wu et al., 2011). In this sense, picture naming task might provide additional information on the relationship between HGA and BOLD responses.

HGAs, which seem to reflect the excitement of local neural assemblies, are only a part of various electrical activities generated in a human brain. Although we mainly investigated the HGA as a plausible candidate of electrophysiological correlates for BOLD responses, some parts of the BOLD responses could be attributable to the power changes in other frequency ranges. Scheeringa et al. (2011) performed simultaneous recording of EEG and fMRI and found that gamma power increase and alpha-beta power decrease in EEG were positively and negatively correlated with BOLD responses in the primary visual area, respectively (Scheeringa et al., 2011). Hermes et al. (2011), in their study on LFP–BOLD coupling in motor function, suggested that BOLD signal change was largely induced by high gamma power increase and alpha-beta power decrease in the primary motor area. Furthermore, Khursheed et al. (2011) stressed that theta power decrease had the most negative correlation with BOLD responses in working memory on the frontal lobe. On the basis of previous studies and our own, HGA–BOLD coupling is a promising key to identify complex human brain functions. Despite the strong correlation of HGA and BOLD signal in our study, it would be necessary to analyze other frequency ranges of electrical activities for further understanding.

Brain regions might have different hemodynamic responsive function (HRF) according to different tasks (Kruggel and von Cramon, 1999). BOLD responses obtained by block-design fMRI paradigms, however, do not reflect such regional differences of HRF. Most of the previous studies including ours on LFP–BOLD coupling have used block-design paradigms (Hermes et al., 2011; Logothetis et al., 2001; Ojemann et al., 2009) because of the high signal-to-noise ratio. Event-related fMRI paradigms, which can detect transient variations in hemodynamic responses, might allow the temporal characterization of BOLD signal changes. This technique, however, has lower signal-to-noise ratio than the block-design fMRI paradigm in the present system setting. It would be possible to make detailed analysis of the coupling if we were to use novel fMRI techniques with higher signal-to-noise ratio and temporal resolution.

Conclusion

This study provided an important bridge between the functional brain networks revealed by BOLD responses and the underlying neurophysiology. We found that there were different temporal profiles of HGA in the frontal and temporal language areas. The longer-lasting HGA contributed to dominant fMRI activation in the frontal lobe, whereas the short-duration HGA reflected poor BOLD signals in the temporal lobe. Such different temporal patterns of HGAs in each lobe might have generated the different BOLD responses around the functional epicenters, which could have led to the dissociation of the spatial distributions of HGAs and BOLD responses.

We believe this work will facilitate practical utilization of fMRI for evaluating higher-order cognitive functions not only in neuroscience research but also in a clinical context.

References

Arne, E., 2010. How and when the fMRI BOLD signal relates to underlying neural activity: the danger in dissociation. Brain Res. Rev. 62, 233–244.
Attwell, D., Iadecola, C., 2002. The neural basis of functional brain imaging signals. Trends Neurosci. 25, 621–625.
Badre, D., Wagner, A.D., 2007. Left ventrolateral prefrontal cortex and the cognitive control of memory. Neuropsychologia 45, 2883–2901.
Binder, J.R., Desai, R.H., Graves, W.W., Conant, L.L., 2009. Where is the semantic system? A critical review and meta-analysis of 120 functional neuroimaging studies. Cereb. Cortex 19, 2767–2796.
Bizzi, A., Blasi, V., Falini, A., Ferroli, P., Cadioli, M., Danesi, U., Aquino, D., Marras, C., Caldiroli, D., Broggi, G., 2008. Presurgical functional MR imaging of language and motor functions: validation with intraoperative electrocortical mapping. Radiology 248, 579–589.
Brett, M., Anton, J., Valbregue, R., Poline, J., 2002. Region of interest analysis using an SPM toolbox. 8th International Conference on Functional Mapping of the Human Brain, Sendai, Japan.
Cardin, J.A., Carlen, M., Meletis, K., Knoblich, U., Zhang, F., Deisseroth, K., Tsai, L.H., Moore, C.I., 2009. Driving fast-spiking cells induces gamma rhythm and controls sensory responses. Nature 459, 663–667.
Conner, C.R., Ellmore, T.M., Pieters, T.A., DiSano, M.A., Tandon, N., 2011. Variability of the relationship between electrophysiology and BOLD-fMRI across cortical regions in humans. J. Neurosci. 31, 12855–12865.
Fiez, J.A., 1997. Phonology, semantics, and the role of the left inferior prefrontal cortex. Hum. Brain Mapp. 5, 79–83.
Friston, K.J., Holmes, A.P., Poline, J.B., Grasby, P.J., Williams, S.C., Frackowiak, R.S., Turner, R., 1995. Analysis of fMRI time-series revisited. Neuroimage 2, 45–53.
Goense, J.B., Logothetis, N.K., 2008. Neurophysiology of the BOLD fMRI signal in awake monkeys. Curr. Biol. 18, 631–640.
Hermes, D., Miller, K.J., Vansteensel, M.J., Aarnoutse, E.J., Leijten, F.S., Ramsey, N.F., 2011. Neurophysiologic correlates of fMRI in human motor cortex. Hum. Brain Mapp. 33, 1689–1699.
Hormuzdi, S.G., Pais, I., LeBeau, F.E., Towers, S.K., Rozov, A., Buhl, E.H., Whittington, M.A., Monyer, H., 2001. Impaired electrical signaling disrupts gamma frequency oscillations in connexin 36-deficient mice. Neuron 31, 487–495.
Kamada, K., Sawamura, Y., Takeuchi, F., Kuriki, S., Kawai, K., Morita, A., Todo, T., 2007. Expressive and receptive language areas determined by a non-invasive reliable method using functional magnetic resonance imaging and magnetoencephalography. Neurosurgery 60, 296–305 (discussion 305–296).
Khursheed, F., Tandon, N., Tertel, K., Pieters, T.A., Disano, M.A., Ellmore, T.M., 2011. Frequency-specific electrocorticographic correlates of working memory delay period fMRI activity. Neuroimage 56, 1773–1782.
Kruggel, F., von Cramon, D.Y., 1999. Temporal properties of the hemodynamic response in functional MRI. Hum. Brain Mapp. 8, 259–271.
Kunii, N., Kamada, K., Ota, T., Greenblatt, R.E., Kawai, K., Saito, N., in press. The dynamics of language-related high-gamma activity assessed on a spatially-normalized brain. Clin. Neurophysiol. http://dx.doi.org/10.1016/j.clinph.2012.06.006.
Kunii, N., Kamada, K., Ota, T., Kawai, K., Saito, N., 2011. A detailed analysis of functional magnetic resonance imaging in the frontal language area—a comparative study with extraoperative electrocortical stimulation. Neurosurgery 69, 590–596 (discussion 596–597).
Lachaux, J.P., Fonlupt, P., Kahane, P., Minotti, L., Hoffmann, D., Bertrand, O., Baciu, M., 2007. Relationship between task-related gamma oscillations and BOLD signal: new insights from combined fMRI and intracranial EEG. Hum. Brain Mapp. 28, 1368–1375.
Leuthardt, E.C., Miller, K., Anderson, N.R., Schalk, G., Dowling, J., Miller, J., Moran, D.W., Ojemann, J.G., 2007. Electrocorticographic frequency alteration mapping: a clinical technique for mapping the motor cortex. Neurosurgery 60, 260–270 (discussion 270–261).
Logothetis, N.K., Pauls, J., Augath, M., Trinath, T., Oeltermann, A., 2001. Neurophysiological investigation of the basis of the fMRI signal. Nature 412, 150–157.
Martin, A., Haxby, J.V., Lalonde, F.M., Wiggs, C.L., Ungerleider, L.G., 1995. Discrete cortical regions associated with knowledge of color and knowledge of action. Science 270, 102–105.

Martin, A., Wiggs, C.L., Ungerleider, L.G., Haxby, J.V., 1996. Neural correlates of category-specific knowledge. Nature 379, 649–652.

Niessing, J., Ebisch, B., Schmidt, K.E., Niessing, M., Singer, W., Galuske, R.A., 2005. Hemodynamic signals correlate tightly with synchronized gamma oscillations. Science 309, 948–951.

Nir, Y., Fisch, L., Mukamel, R., Gelbard-Sagiv, H., Arieli, A., Fried, I., Malach, R., 2007. Coupling between neuronal firing rate, gamma LFP, and BOLD fMRI is related to interneuronal correlations. Curr. Biol. 17, 1275–1285.

Noppeney, U., Phillips, J., Price, C., 2004. The neural areas that control the retrieval and selection of semantics. Neuropsychologia 42, 1269–1280.

Ogawa, S., Lee, T.M., Kay, A.R., Tank, D.W., 1990. Brain magnetic resonance imaging with contrast dependent on blood oxygenation. Proc. Natl. Acad. Sci. U. S. A. 87, 9868–9872.

Ojemann, G.A., Corina, D.P., Corrigan, N., Schoenfield-McNeill, J., Poliakov, A., Zamora, L., Zanos, S., 2009. Neuronal correlates of functional magnetic resonance imaging in human temporal cortex. Brain 133, 46–59.

Ossadtchi, A., Greenblatt, R.E., Towle, V.L., Kohrman, M.H., Kamada, K., 2010. Inferring spatiotemporal network patterns from intracranial EEG data. Clin. Neurophysiol. 121, 823–835.

Price, C.J., 2012. A review and synthesis of the first 20 years of PET and fMRI studies of heard speech, spoken language and reading. Neuroimage 62, 816–847.

Rutten, G.J., Ramsey, N.F., van Rijen, P.C., Noordmans, H.J., van Veelen, C.W., 2002. Development of a functional magnetic resonance imaging protocol for intraoperative localization of critical temporoparietal language areas. Ann. Neurol. 51, 350–360.

Scheeringa, R., Fries, P., Petersson, K.M., Oostenveld, R., Grothe, I., Norris, D.G., Hagoort, P., Bastiaansen, M.C., 2011. Neuronal dynamics underlying high- and low-frequency EEG oscillations contribute independently to the human BOLD signal. Neuron 69, 572–583.

Thompson-Schill, S.L., D'Esposito, M., Aguirre, G.K., Farah, M.J., 1997. Role of left inferior prefrontal cortex in retrieval of semantic knowledge: a reevaluation. Proc. Natl. Acad. Sci. U. S. A. 94, 14792–14797.

Traub, R.D., Jefferys, J.G., Whittington, M.A., 1997. Simulation of gamma rhythms in networks of interneurons and pyramidal cells. J. Comput. Neurosci. 4, 141–150.

Traub, R.D., Kopell, N., Bibbig, A., Buhl, E.H., LeBeau, F.E., Whittington, M.A., 2001. Gap junctions between interneuron dendrites can enhance synchrony of gamma oscillations in distributed networks. J. Neurosci. 21, 9478–9486.

Veltman, D.J., Friston, K.J., Sanders, G., Price, C.J., 2000. Regionally specific sensitivity differences in fMRI and PET: where do they come from? Neuroimage 11, 575–588.

Wagner, A.D., Pare-Blagoev, E.J., Clark, J., Poldrack, R.A., 2001. Recovering meaning: left prefrontal cortex guides controlled semantic retrieval. Neuron 31, 329–338.

Wang, X.J., Buzsaki, G., 1996. Gamma oscillation by synaptic inhibition in a hippocampal interneuronal network model. J. Neurosci. 16, 6402–6413.

Wu, H.C., Nagasawa, T., Brown, E.C., Juhasz, C., Rothermel, R., Hoechstetter, K., Shah, A., Mittal, S., Fuerst, D., Sood, S., Asano, E., 2011. Gamma-oscillations modulated by picture naming and word reading: intracranial recording in epileptic patients. Clin. Neurophysiol. 122, 1929–1942.
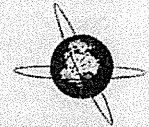
The dynamics of language-related high-gamma activity assessed on a spatially-normalized brain

Naoto Kunii [a], Kyousuke Kamada [b,*], Takahiro Ota [a], Richard E. Greenblatt [c], Kensuke Kawai [a], Nobuhito Saito [a]

[a] Department of Neurosurgery, The University of Tokyo, Tokyo, Japan
[b] Department of Neurosurgery, Asahikawa Medical University, Asahikawa, Japan
[c] Source Signal Imaging Inc., San Diego, CA, USA

ARTICLE INFO

HIGHLIGHTS

- We made spatial normalization of 1512 intracranial electrodes in 21 patients with intractable epilepsy to identify typical dynamics of semantic processing.
- Word interpretation task evoked high gamma activity (HGA) at 200 ms after stimulus onset on the posterior temporal language area and alternatively at 400 ms on the frontal language area, following the initial HGA of bilateral fusiform gyri.
- The novel ECoG-normalization technique evolved visualization of electrophysiological dynamics related to semantic processing among individual subjects.

ABSTRACT

Objective: We developed a novel technique of spatial normalization of subdural electrode positions across subjects and assessed the spatial–temporal dynamics of high-gamma activity (HGA) in the dominant hemisphere elicited by three distinct language tasks.
Methods: The normalization process was applied to 1512 subdural electrodes implanted in 21 patients with intractable epilepsy. We projected each task-related HGA profile onto a normalized brain.
Results: The word interpretation task initially elicited HGA augmentation in the bilateral fusiform gyri at 100 ms after stimulus onsets, subsequently in the left posterior middle temporal gyrus, in the left ventral premotor cortex at 200 ms and in the left middle and left inferior frontal gyri at 300 ms and after. The picture naming task elicited HGA augmentation in few sites in the left frontal lobe. The verb generation task elicited HGA in the left superior temporal gyrus at 100–600 ms. Common HGA augmentation elicited by all three tasks was noted in the left posterior-middle temporal and left ventral premotor cortices.
Conclusions: The spatial–temporal dynamics of language-related HGA were demonstrated on a spatially-normalized brain template.
Significance: This study externally validated the spatial and temporal dynamics of language processing suggested by previous neuroimaging and electrophysiological studies.
© 2012 International Federation of Clinical Neurophysiology. Published by Elsevier Ireland Ltd. All rights reserved.

1. Introduction

Language functions are generated by complex neural networks. To obtain better understanding of language mechanisms, it is necessary to make detailed maps using functional imaging and electrophysiological techniques. In particular, fine-scale time series analysis of the whole brain has great potential for the elucidation of neural networks.

Numerous lesional and hemodynamic studies have provided information about language networks (Binder et al., 2009; Dronkers et al., 2004; Price, 2010; Vigneau et al., 2006). In addition to the classical Wernicke's and Broca's areas, recent studies have found several language-related epicenters throughout the whole brain. The regions that are activated depend on the cognitive function being performed, for example, various areas of the brain have been found to be associated with orthography (Binder et al., 2006; Cohen et al., 2002; Tsapkini and Rapp, 2010), phonology (Binder et al., 2000; Buchsbaum et al., 2001; Rauschecker, 1998),

* Corresponding author. Address: Department of Neurosurgery, Asahikawa Medical University, 2-1, Midorigaoka-Higashi, Asahikawa, Hokkaido 078-8510, Japan. Tel.: +81 166 68 2594; fax: +81 166 68 2599.
E-mail address: kamady-k@umin.ac.jp (K. Kamada).

lexico-semantic memory (Martin et al., 1995, 1996; Moore and Price, 1999; Noppeney et al., 2005), semantic selection/decisions (Badre and Wagner, 2007; Noppeney et al., 2004; Thompson-Schill et al., 1999; Wagner et al., 2001), speech production/perception (D'Ausilio et al., 2009; Hickok, 2001; Hickok et al., 2003; Pulvermuller et al., 2006; Wilson et al., 2004), syntax and sentence level comprehension (Friederici et al., 2003; Hashimoto and Sakai, 2002; Homae et al., 2002, 2003; Humphries et al., 2001; Ni et al., 2000), and verbal working memory (Champod and Petrides, 2007, 2010; Hickok et al., 2003; Jonides et al., 1998; Ravizza et al., 2004; Tsukiura et al., 2001). Although multiple epicenters have been found, it is difficult to elucidate the time course of the brain activity of distributed language areas and the dynamics of the language network. This is due to the technical limitations of hemodynamic studies such as positron emission computed tomography (PET) and functional MRI (fMRI), which have insufficient temporal resolution to describe the dynamics of neural activity.

On the other hand, electroencephalography (EEG) and magnetoencephalography (MEG) have been used to record event-related responses at high time resolution; i.e., event-related potentials (ERP) and event-related fields (ERF), respectively. Using these techniques, previous groups have demonstrated semantic responses within 200 ms of letter presentation for primary perception and within about 400 ms for letter cognition (Dhond et al., 2007; Salmelin et al., 1994; Vartiainen et al., 2009). However, questions remain about how to solve inverse problems, which interfere with source localization. In fact, there have been considerable disagreements about the origins of certain components (e.g., N400) (Curran et al., 1993; Halgren et al., 2002; Helenius et al., 1998; Johnson and Hamm, 2000; Maess et al., 2006; Pylkkanen and McElree, 2007; Tse et al., 2007; Uusvuori et al., 2008).

In the last few years, increasing effort has been made to assess brain oscillatory activity such as event-related synchro/desynchronization (ERS/ERD) using intracranial electrodes. Event-related augmentation of the ongoing EEG has been referred to as ERS, and augmentation of high gamma activity (HGA) at >50 Hz is generally considered to reflect cortical activation (Crone et al., 1998; Pfurtscheller and Lopes da Silva 1999).

Distributions of HGA augmentation display strong correlations with various functions, including motor (Crone et al., 1998; Leuthardt et al., 2007; Miller et al., 2007), auditory (Crone et al., 2001a; Edwards et al., 2005; Sinai et al., 2009; Trautner et al., 2006), visual (Lachaux et al., 2005; Tanji et al., 2005), language (Brown et al., 2008; Crone et al., 2001b; Sinai et al., 2005; Wu et al., 2011, 2010), episodic memory (Sederberg et al., 2007), working memory (Axmacher et al., 2007; Howard et al., 2003; Meltzer et al., 2008; van Vugt et al., 2010), and attention functions (Jung et al., 2008; Ray et al., 2008; Tallon-Baudry et al., 2005). Furthermore, studies of HGA can achieve both high spatial and temporal resolution. Therefore, analyzing HGA dynamics is one of the most powerful approaches for studying complex neural networks (Canolty et al., 2007; Edwards et al., 2010; Mainy et al., 2008).

One practical issue with this technique is the positioning of intracranial electrodes. Since it is impossible to control the electrode positions for research purposes from an ethical point of view, each patient is monitored with a different number of electrodes, and there are also inter-individual differences in their locations. As a result, consistent HGA dynamics are rarely obtained because of inter-individual variations in electrode positioning.

In order to overcome these limitations, we spatially normalized individual brains and the subdural electrodes of patients with intractable epilepsy and superimposed 1512 electrodes of the dominant hemisphere onto a normalized brain. We hypothesized that this novel method could allow us to demonstrate representative HGA patterns for various semantic tasks such as word interpretation, picture naming, and verb generation.

2. Subjects and methods

2.1. Subjects

We recorded ECoG in 34 patients with intractable epilepsy, who underwent subdural electrode implantation for diagnostic purposes at the University of Tokyo Hospital between May 2005 and November 2010. During the recording, we instructed the patients to perform 3 language tasks, word interpretation, picture naming, and verb generation. Thirteen patients were excluded because of a low intelligence quotient (<70) ($n = 9$), young age (<15) ($n = 1$), a lack of electrodes in the left hemisphere ($n = 1$), low signal quality ($n = 1$), or continuous epileptic activity ($n = 1$). As a result, we restricted this analysis to 21 patients (8 men, 13 women). Before the epilepsy surgery, we confirmed which hemisphere was dominant for language processes in each individual using the Wada test or a combination of fMRI and MEG, as described elsewhere (Kamada et al., 2007). There was no case in which the right hemisphere was dominant for language processes.

We used grid and strip type subdural electrodes, which consisted of silastic sheets embedded with platinum electrodes (3 mm in diameter), and a 10 mm inter-electrode interval (center to center) (Unique Medical, Tokyo, Japan). Since the purpose of this study was to elucidate the language dynamics in the dominant hemisphere, we excluded ECoG electrodes on the lateral surface of the right hemisphere.

This study was approved by the institutional review board of our institute. Written informed consent was obtained from each patient or their family after a detailed explanation of the ECoG and language evaluation procedures.

2.2. ECoG recording

2.2.1. Data acquisition

Each patient was seated on a bed with a reclining backrest in a quiet, electrically shielded room. A computer monitor was placed 100 cm from the patient. Stimuli were then presented using a Stimuli Output Sequencer (NoruPro Light Systems Inc., Tokyo, Japan).

The resultant ECoG were digitally recorded at a sampling rate of 400 Hz, using a 128 channel EEG system (BMSI 6000, Nicolet Biomedical Inc., Wisconsin). The band-pass filter for the data acquisition was set to 0.55–150 Hz. Electric triggers generated by the stimulus computer were simultaneously recorded by one of the channels.

A reference electrode was placed on the scalp at Cz (international 10–20 system).

2.2.2. Language tasks

Word interpretation (WI) task: The stimuli for the word interpretation task consisted of three-letter words. All letter strings were white with a black background and presented for 350 ms with a randomly variable inter-stimulus intervals, ranging between 2700 and 3300 ms. The words were displayed randomly, and each was presented once or twice, yielding 100 data epochs. The patients were instructed to covertly categorize the presented words into "abstract" or "concrete".

Picture naming (PN) task: The 100 stimuli used for the picture naming task consisted of 42 color illustrations of familiar objects. They were presented for 1000 ms with an inter-stimulus interval ranging between 2700 and 3300 ms. The patient was requested to silently name each presented object.

Verb generation (VG) task: Common concrete nouns spoken by a native Japanese speaker were presented by the computer. The twenty stimuli were presented in random order to generate 100

data epochs. The duration range of the auditory stimuli was <500 ms, and the inter-stimulus intervals varied randomly from 2700 to 3300 ms. The patient was instructed to silently generate a verb related to each presented noun.

2.3. Data analysis

2.3.1. ECoG data processing

All analyses of the ECoG data were performed using custom software written in Matlab R2008b (The Mathworks, Inc., Natick, MA). We divided the continuous ECoG into 2 s epochs (0.5 s before and 1.5 s after stimulus onset) with an additional 0.125 s on both sides of each epoch to prevent 'edge effect' artifacts from clouding the results. Based on a visual inspection of the ECoG signals, trials involving excessive epileptic activity were excluded from further analysis.

2.3.2. Time–frequency analysis

We used spectrograms to estimate the energy density of the signals in the time–frequency plane (Makeig, 1993; Zygierewicz et al., 2005), as described below: We divided the signal, $s(t)$, into overlapping epochs, each of which was multiplied by the window-function $w(t)$. Then, the Fourier transformation was performed on the windowed epochs, providing a frequency resolution dependent on the epoch length. The short-time Fourier transform (STFT) of signal $s(t)$ was given by:

$$F_s(u,f) \int_{-\infty}^{\infty} s(t)\omega^*(t-u)e^{-2\pi ift} dt \tag{1}$$

We used the following Hamming window:

$$w(t) = 0.54 - 0.46\cos\left(2\pi\frac{t}{T}\right) \tag{2}$$

where T was the window length. We then obtained a spectrogram by squaring the modulus of the STFT.

Each epoch of 800 time points was comprised of 80 Hamming-windowed, 100-point data windows with 90% overlap. For spectral interpolation, we applied zero-padding to the windowed time series, thus the output consisted of 100 frequency bins with width of 2 Hz. As a result, we obtained N time–frequency power distribution maps composed of 100 frequency bins, each of which was derived from 20 pre-stimulus and 60 post-stimulus time-series data points, where N represented the number of trials for each task.

2.3.3. Permutation test

We performed a permutation test to determine P values for each time–frequency point under the null hypothesis that there is no difference between the power value at a post-stimulus time–frequency point and the mean power value of the same frequency bin at the pre-stimulus baseline. The P value for each time–frequency point was obtained as follows (see Appendix A for more detail).

N mean power values at the pre-stimulus baseline and N time–frequency power values at a post-stimulus time–frequency point were pooled together and then 999 iterations were randomly shuffled and partitioned into two series of the same size as the original series. Averaging these shuffled series generated a probability distribution of power values at each time–frequency point. For each time–frequency point, raw P values were obtained as percentiles within this distribution (P value resolution of 0.001).

2.3.4. FDR analysis

We corrected the obtained P values for multiple comparisons using the false discovery rate (FDR) method (Benjamini and Hochberg, 1995; Genovese et al., 2002; Ray et al., 2008). This procedure controls for the expected proportion of falsely rejected hypotheses. Using the P values of a given frequency bin, the FDR method was used to find an appropriate significance level below which all time points were considered significant. First, all the P values of the frequency bin (the number of time points was B) were ordered from smallest to largest (denoted by $P(i)$, $i = 1, 2, \ldots, B$). The cut-off level was then given by $P(r)$, where r was the largest i such that

$$\tilde{P}(i) \le i \times \frac{q}{B} . \tag{3}$$

where q was the desired FDR (set to 0.05 in this paper). This procedure was repeated for each frequency, yielding a time–frequency map corrected for multiple comparisons in the time domain.

2.3.5. Quantification of high gamma activity

The definition of the high gamma frequency band differed among previous studies. Although the full HGA ranges from 50–150 Hz, only the range from 60 to 120 Hz was used in order to avoid electrical artifacts at 50 and 150 Hz and because this is the frequency range in which the maximal response was obtained. Within this frequency range, we counted the number of frequency bins that displayed significant augmentation at each time point. We termed the resultant number the high gamma broadband index (HGBI). A HGBI of 1.0 or 0 at a given channel indicates all or no bins were significantly increased over whole high gamma frequency band, respectively. A HGBI of 0.5 corresponds to 50% of bins with significant increase.

2.4. Brain normalization

2.4.1. Visualization of spatially normalized channel activity

Anatomical brain images and the positions of the implanted electrode were obtained by preoperative three-dimensional T1-weighted imaging (3D MRI) and 3D CT performed after electrode implantation, respectively. The 3D CT data was then co-registered with the 3D MRI data by maximizing the mutual information between the two datasets. The co-registered 3D-CT was interpolated and re-sliced according to the header information of the 3D-MRI using Dr. View (Asahi Kasei, Tokyo, Japan).

The dataset for the 3D-MRI and the resliced 3D-CT data were imported into SPM8 in ANALYZE format (Welcome Department of Imaging Neuroscience, London, UK; www.fil.ion.ucl.ac.uk/spm). The 3D-MRI of each patient was normalized to the equipped T1-template and converted to Montreal Neurological Institute coordinate space. Each re-sliced 3D-CT dataset was also normalized using the same parameters as were used for the 3D-MRI normalization. After the data conversion, we selected a patient's brain as a repre-

Electrode distribution
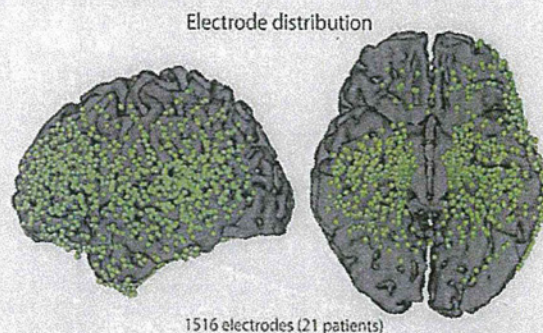
1516 electrodes (21 patients)

Fig. 1. Electrode distribution. The normalized electrodes were illustrated as green dots in the lateral (left) and basal (right) aspects of the template brain. The electrode positions of each patient were derived from the three-dimensional computed tomography datasets.

sentative brain model and superimposed the electrodes of all patients onto it.

The representative MRI and normalized CT sets of all patients were imported into EMSE (Source Signal Imaging, San Diego, CA) (Ossadtchi et al., 2010). Each electrode location was digitized semi-automatically using predefined electrode templates. EMSE automatically bent the digitized templates to fit the electrodes to the brain surface. Although this procedure carried a risk of registration errors, we compared the results and intraoperative findings during electrode implantation and removal and found that there was little difference between them. We registered the ECoG channels of all patients to the corresponding digitized electrodes (Fig. 1A).

2.4.2. Electrode density correction

To avoid overestimating the HGBI in areas of high electrode density, each HGBI was corrected for the electrode density of the corresponding area by dividing the HGBI by the number of electrodes within 5 mm of each electrode center (cHGBI). cHGBI time series for each channel were displayed on the normalized brain surface using Gaussian interpolation with a sigma value of 10 mm.

2.5. Time series analysis using VOI

We performed volume-of-interest (VOI) analysis to provide quantitative evaluations of HGA dynamics. VOI were assigned to 6 areas that showed representative HGA profiles.

The HGBI of all the electrodes inside each VOI were averaged to show temporal changes. We used a 15 mm VOI radius to prevent overlapping among VOI. For the three language tasks, we used the same set of VOI to enable comparisons among the HGA dynamics of different tasks. If the averaged HGBI in a given VOI corresponded to 1.0, it means all time–frequency bins at all electrodes in the VOI showed a significant increase in high gamma frequency band. The HGBI values in the VOI analysis, therefore, depended not only on the degree of HGA, but also on the number of electrodes which showed strong HGA augmentation.

3. Results

3.1. Summary of the normalized data

The number of patients and electrodes investigated for each task were as follows: the WI task was performed in 21 patients with 1516 electrodes, and the VG and PN tasks were performed in 12 patients with 884 electrodes and 14 patients with 1048 electrodes, respectively. The demographic data of each task group are summarized in Table 1. There was no significant difference be-

Table 1
Demographic data of each task group.

	WI	PN	VG	P value
No. of patients	21	14	12	
Age	32.4 + −8.95	32.5 + −8.9	32.8 + −9.6	0.99[a]
Sex (M/F)	0.62	0.80	0.50	0.88[b]
Epilepsy onset	17.3 + −10.0	17.6 + −11.0	20.9 + −10.0	0.61[a]
Epilepsy duration	15.0 + −11.4	14.9 + −10.9	11.9 + −9.4	0.70[a]
Epilepsy side (L/R)	1.5	1.8	1.2	0.89[b]
No. of electrodes (base)	33.0 + −6.3	34.9 + −6.1	31.2 + −5.1	0.30[a]
No. of electrodes (Left)	39.2 + −15.1	40.0 + −12.3	42.5 + −17.9	0.83[a]
VIQ	86.8 + −9.6	88.9 + −9.6	87.8 + −9.1	0.81[a]

WI = word interpretation; PN = picture naming; VG = verb generation; VIQ = verbal intelligence quotient.
[a] One-way ANOVA.
[b] Chi-square test.
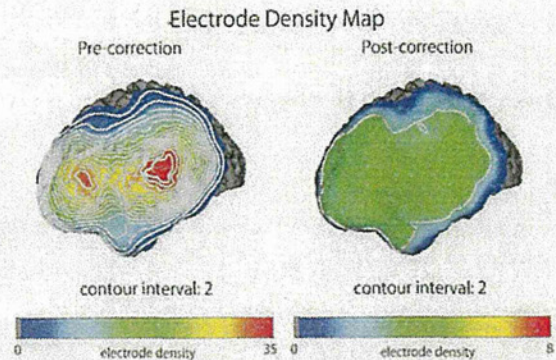
Electrode Density Map

Fig. 2. Electrode density map. Before the correction of electrode density (left), there was high concentration of electrodes in Broca's and Wernicke's areas, reflecting the clinical importance of these areas. The correction resulted in the electrode density becoming almost uniform (right), eliminating the effect of electrode density on the visualization of high gamma activity.

tween the background data of any group. The normalized electrodes were found to cover an extensive range of the lateral frontotemporal lobes and the basal aspect of the occipitotemporal areas (Fig 1). The distribution of electrodes was similar among the three groups (data not shown).

3.2. Electrode density correction

We created electrode density maps to evaluate the heterogeneity of electrode density. Before correction, the electrode density was relatively high in the classical Broca's and Wernicke's areas (Fig. 2A). The correction resulted in the electrode density becoming homogenous throughout the areas covered by the electrodes and was effective at removing the observed electrode density heterogeneity (Fig. 2B).

3.3. Dynamics

We projected cHGBI values onto the brain surface for each language task (Figs. 3–5A).

3.3.1. Spatial distributions of HGA in different tasks

As no electrodes were located in the calcarine fissure, we did not observe the primary responses to the visual stimuli. In the WI task, following the initial recruitment of the bilateral FuG, HGA augmentation in the posterior middle temporal gyrus (pMTG) was observed. In addition, sustained augmentation of HGA was seen over the ventral premotor cortex (vPMC). The latest recruitment occurred over the middle frontal gyrus (MFG) and inferior frontal gyrus (IFG) (Fig. 3A).

Although the dynamics of the PN were similar to those of the WI, the bilateral FuG was more widely involved. Another unique finding was that there was little HGA augmentation in the MFG or IFG during the PN (Fig. 4A).

Since the VG task used auditory stimuli, HGA augmentation was mainly observed in the lateral aspect of the superior temporal gyrus (STG), with no response seen in the basal aspects of bilateral temporal lobes. Subsequently, the pMTG showed HGA augmentation to a similar degree to that seen during the other two tasks. On the other hand, the vPMC displayed slow-onset recruitment. HGA augmentation in the MFG and IFG were maintained until 1000 ms after the VG stimuli, which were similar to those observed during the WI processing (Fig. 5A).
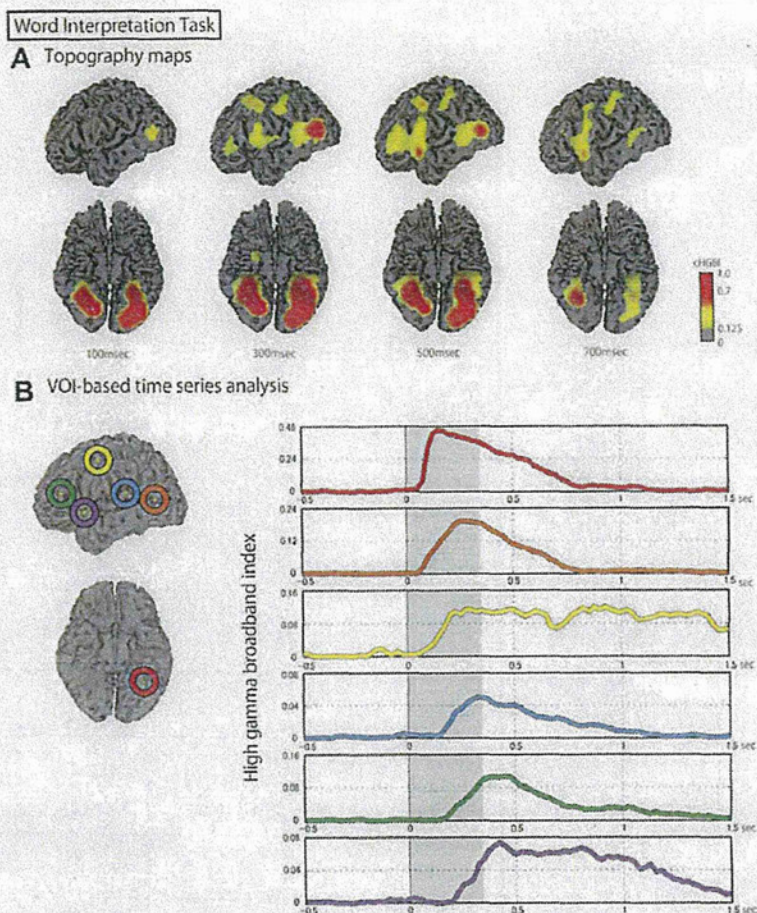
Fig. 3. Word interpretation results. (A) Topographic maps of the high gamma broadband index values (HGBI with electrode density correction) for the word interpretation task. HGBI profiles were aligned on the brain surface at representative time points, indicating sequential activation of the fusiform gyrus (FuG), posterior middle temporal gyrus (pMTG), ventral premotor cortex (vPMC), and middle and inferior frontal gyri (MFG and IFG). (B) HGBI time series of each volume of interest (VOI). The VOI included the FuG (Red), pMTG (Orange), vPMC (Yellow), the superior temporal gyrus (Blue), and the MFG (Green) and IFG (Purple). Each VOI and the corresponding HGBI line are shown in the same color. The gray zones indicate the duration of stimulus presentation. Note the differences in the vertical axis scales among different VOI.

3.3.2. VOI-based time series analysis of HGA during different tasks

To quantitatively evaluate HGA dynamics, we set VOI (radius 15 mm) in the following six cortical areas: FuG, pMTG, STG, vPMC, MFG, and IFG. These areas were chosen because they demonstrated marked HGA augmentation. Figs. 3–5B illustrates the time courses of the averaged raw HGBI within each VOI for each task.

In the WI task, HGA augmentation in the FuG occurred first, beginning at around 100 ms, and the pMTG was recruited slightly later. The FuG augmentation declined after the termination of the visual stimuli, while the vPMC displayed prolonged response between 200 and 1000 ms. Both the MFG and IFG were involved at around 300 ms. The MFG augmentation rapidly decreased at around 400 ms, whereas the IFG augmentation was sustained until 1000 ms (Fig. 3B).

In the PN task, the FuG augmentation occurred first, beginning at around 100 ms and was sustained for more than 1000 ms, reflecting the longer stimulus presentation time of this task. On the other hand, the HGA augmentation of the pMTG occurred slightly later than that observed during the WI; i.e., from 200 ms to 700 ms. The vPMC showed prolonged augmentation between 300 and 900 ms during the PN task, which was similar to that seen

during the WI task. The MFG and IFG demonstrated low HGBI values during this task (Fig. 4B).

The initial response related to the VG task involved prominent HGA augmentation of the STG between 100 and 600 ms. The next peaks appeared simultaneously in the pMTG, IFG, and MFG and then gradually decreased until 1000 ms. An interesting characteristic of the HGBI profile for this task was late onset of vPMC response, which appeared at around 500 ms and peaked at around 1000 ms (Fig. 5B).

VOI-based time series analysis demonstrated different HGBI profiles for each task.

4. Discussion

We demonstrated the spatiotemporal dynamics of the brain oscillations related to three different language tasks using a novel method in which we superimposed ECoG-HGA from 21 patients onto a normalized brain. The HGA-dynamics for the WI task demonstrated posterior-to-anterior sequences of cortical recruitment involving the FuG, pMTG, vPMC, MFG, and IFG. Although similar dynamics was observed during the PN task, little HGA was ob-
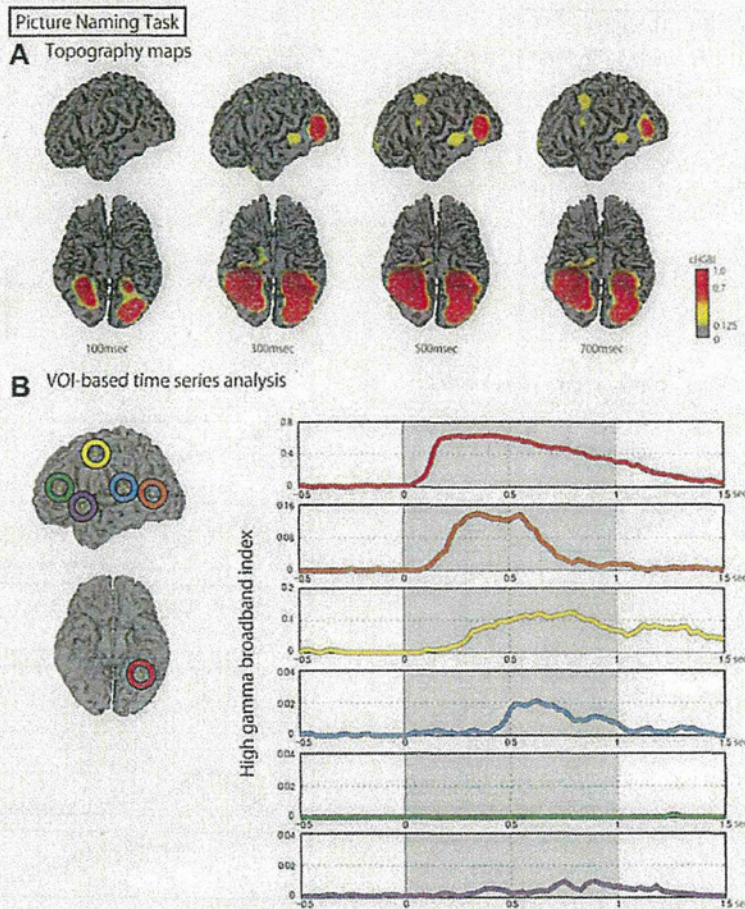
Fig. 4. Picture naming results. The plotting conventions were the same as those employed for Fig. 3. There were marked activations in the bilateral fusiform gyri. The posterior middle temporal gyrus and ventral premotor cortex showed similar dynamics to those observed during the word interpretation task. In contrast to the word interpretation task, the picture naming task induced little activation in the frontal lobe.

served over the MFG-IFG region. The VG task widely activated the STG instead of the FuG between 100 and 600 ms after the presentation of auditory stimuli. The HGA produced in the IFG during the VG task was stronger than those observed during the WI and PN tasks, although similar HGA-propagations were seen in other areas. This report presented a novel technique of ECoG visualization and successfully elucidated typical HGA profiles for different language processes.

Neuroimaging studies have accumulated knowledge about the putative roles of distributed cortical areas. Since WI task used in this study could be achieved only through covertly reading the visually presented words, it seems reasonable to discuss its processing in the context of reading function. In previous studies of the functional areas implicated in word reading, posterior-to-anterior streams of cortical recruitment have generally been described. After the perception of visual stimuli, the FuG is activated during orthographic cognition (Binder et al., 2006; Cohen et al., 2002; Dehaene et al., 2005; Tsapkini and Rapp, 2010). The pMTG is related to lexico-semantic knowledge, and the IFG plays more executive roles in semantic decisions (Badre and Wagner, 2007; Binder et al., 2009; Fiez, 1997; Martin et al., 1995, 1996; Noppeney et al., 2004; Thompson-Schill et al., 1997; Wagner et al., 2001). The WI task used in this study activated these epicenters, and we successfully visualized the sequential activation of each of the

abovementioned brain regions. We believe that our findings support the classical model of reading dynamics.

Picture naming is a common language task employed in neurosurgical language mapping (Ojemann et al., 1989; Penfield and Roberts, 1959; Sinai et al., 2005). However, this task did not activate frontal language areas as strongly as categorization or verb generation tasks in fMRI studies (Herholz et al., 1997; Kunii et al., 2011). In general, picture naming has one correct answer. On the contrary, categorization and verb generation tasks require more executive-level semantic judgment or selection (Edwards et al., 2010; Thompson-Schill et al., 1998), which might account for the stronger activation in the frontal language areas. Our results are consistent with this interpretation as the PN task induced little activation in the IFG or MFG in contrast to the WI task. Several previous fMRI studies showed that naming elicited greater cortical activation in the IFG or MFG than word reading task (MacDonald et al., 2000; Polk et al., 2008). Wu et al. directly compared picture naming with word reading task in their ECoG study and found picture naming task demonstrated wider frontal lobe activation (Wu et al., 2011). We assume that the lack of frontal lobe activation in these studies came from passive reading tasks in contrast to our study, which required semantic decision. This suggests that performing the PN task alone in clinical situations carries a risk of underestimating the cortical areas involved in semantic decision-making.
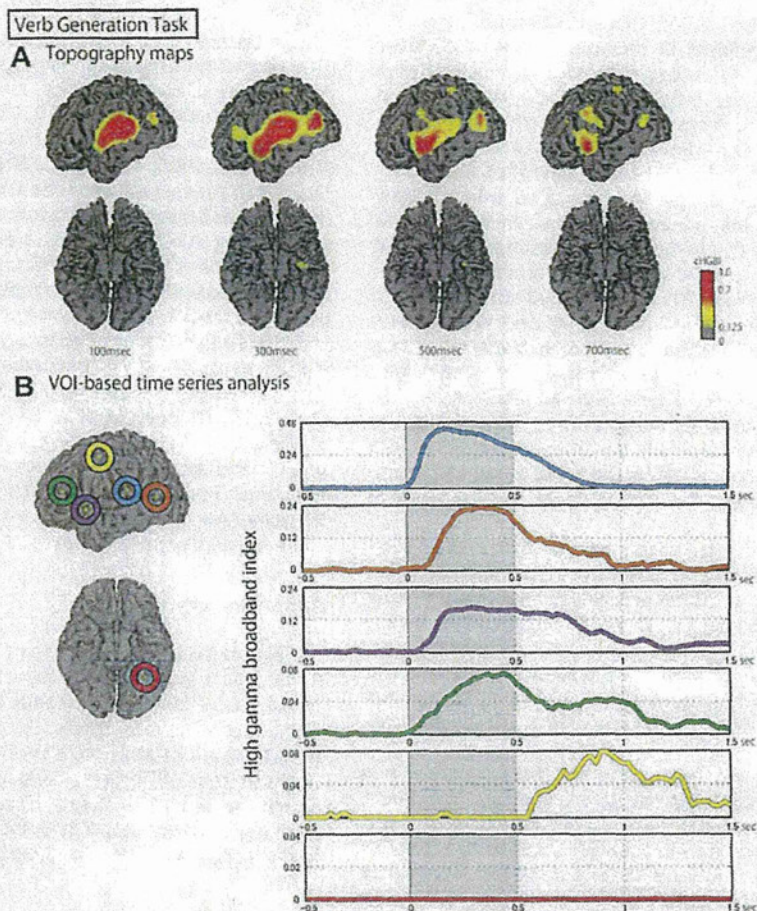
Verb Generation Task

A Topography maps

B VOI-based time series analysis

Fig. 5. Verb generation results. The plotting conventions were the same as those employed for Fig. 3. The auditory stimuli resulted in initial activation of the superior temporal gyrus, followed by the recruitment of the posterior middle temporal gyrus. Activation of the ventral premotor cortex occurred later than in the word interpretation and picture naming tasks. The prolonged recruitment observed in the inferior frontal gyrus was as marked as that in the word interpretation task.

In the VG task, our most remarkable finding was the strong activity in the STG and IFG. Several studies have suggested that the STG responds best to the complex spectro-temporal signals, such as speech, that comprise the higher levels of the cortical auditory processing hierarchy (Binder et al., 2000; Hickok and Poeppel, 2004; Scott et al., 2000). As described above, the IFG plays executive roles in semantic decision-making. The VG task involved selecting one of generated words, which might require complex semantic decision-making in the IFG. These task-dependent characteristics might have generated the characteristic activation patterns observed during the VG task.

We observed two cortical areas that were commonly recruited during language processing. The pMTG was activated not only by visual tasks, but also by auditory tasks, soon after the initial integrative perception in the FuG and STG, respectively. This suggests that the pMTG plays a modality-independent role in various semantic processes. It seems quite reasonable that semantic knowledge is stored in the pMTG irrespective of the input modality due to its storage capacity.

The vPMC was also commonly activated by the three tasks. It was suggested that the vPMC might be involved in imagery articulation during silent rehearsal (Vigneau et al., 2006; Wilson et al., 2004), which could be used to ensure that the verbal working memory remains active (Baddeley, 1992; Baddeley and Hitch,

1974; Hickok and Poeppel, 2004). Furthermore, Duffau et al. (2003) suggested that the functional role of the vPMC involved articulation planning by observing language impairment using electrical stimulation of the vPMC. Our results support the assertion that the vPMC plays an important role in basic language functions such as reading, naming, and listening.

Three human ECoG studies have described the HGA dynamics involved in language processing (Canolty et al., 2007; Edwards et al., 2010; Mainy et al., 2008; Pei et al., 2011). Canolty et al. examined 256 subdural electrode channels in 4 epilepsy patients and provided detailed ECoG dynamics for auditory word processing in the temporal lobe. They demonstrated the sequential activation of the posterior STG, middle STG, and superior temporal sulcus, which added temporal information to functional knowledge of these areas gathered by previous studies.

Mainy et al. performed intracranial EEG using 300 depth electrode channels in 10 epilepsy patients. They observed initial gamma-band activation in the mesial basal temporal lobe at 150 ms, which reached the word form area in the mid fusiform gyrus at 200 ms after word reading. Task specific gamma-band activations were then observed after 400 ms in the superior temporal gyrus for both word and pseudo-word stimuli; in the pars triangularis for word categorization and in the pars opercularis for phonological decision-making. Although the brain areas covered by their

study were subject to practical limitations, they successfully demonstrated consistent dynamics in the frontotemporal language areas across individuals. Our study succeeded in superimposing brain activity data from more than 1500 ECoG-channels onto a normalized brain, which demonstrated similar activation patterns, including visual processing in the fusiform gyrus at around 200 ms and semantic processing in the pars triangularis after 400 ms.

Edward et al. investigated 4 patients with ECoG, using auditory verb generation and picture naming tasks. Their individual ECoG analyses clearly showed that in the verb generation task the initial gamma band activation occurred in the pSTG at around 100 ms, before rapidly moving to the pMTG at around 300 ms. After speech perception, activations for semantic processing were detected over the IFG and MFG. It is worth noting that the verb generation task activated the IFG and MFG significantly more than the picture naming task. Despite the limited number of patients in their study, the time course of cortical activation showed close similarities with the HGA dynamics observed in our study. Edward et al. also referred to the contribution made by the vPMC to speech perception. We strongly agree that the vPMC plays an important role in language tasks.

Pei et al. recently reported spatiotemporal dynamics of ECoG HGA during overt and covert word repetition. Although the investigation was limited to the lateral parasylvian area, they projected each electrodes from 8 subjects onto the template brain for the first time and presented comprehensive characterization of overt and covert speech. They also related the results to the temporal envelope of auditory stimulation and the subject's verbal response. Their study reinforced the important role of HGA as a general index of cortical activation.

The novel achievement of this study was that we were able to normalize all of the ECoG electrode positions of the 21 patients, thereby avoiding inter-individual variability in the obtained spatial and temporal ECoG profiles. Although we acknowledge that this method carries a risk of underestimating weak and inconsistent HGA, it emphasizes the prominent hot spots related to language processing and is helpful for understanding the mechanisms underlying language functions. It is important to note that the spatial comparison of this study was not statistically validated, which implies spatially non-stationary correlation structure of the observed activity. It would be necessary to address the methodological issue for future studies.

In this study, we observed little activation in the angular gyrus or anterior temporal area even though they are considered to be language related areas. Both areas have been suggested to play a role in integrating individual concepts into a larger whole and in sentence-level comprehension (Friederici et al., 2003; Hickok and Poeppel, 2007; Humphries et al., 2001; Newman et al., 2003; Ni et al., 2000). In this report, we made the tasks as easy as possible, since single object processing might be appropriate for functional normalization among patients with a variety of attention levels. In order to identify additional language areas, we might need to use more complex tasks such as sentence comprehension. On the other hand, the anterior medial temporal region seems to show HGA augmentation at around 300 ms in WI and PN tasks. Given that such augmentation was not observed in VG task; this could be attributed to artifacts elicited by fixational eye movements (Nagasawa et al., 2011; Yuval-Greenberg et al., 2008).

Electrode shifts are one of the crucial issues affecting ECoG research (Laviolette et al., 2011). Estimation errors related to electrode localization are also inevitable at each step of normalization, digitization, and registration. In our study, we confirmed the electrode locations in the 2nd operation and that the normalized electrodes produced using SPM8 uniformly covered the language-related areas. As a result, a large number of the electrodes (more than 1500 channels) showed representative HGA

dynamics for each semantic task, which suggests that this method has great potential for improving our understanding of the underlying physiology supporting language functions. Another issue is the reference electrode position, that is Cz in all patients. Thus, high-gamma activity generated by the superior midline region on either hemisphere might contaminate ECoG data at all channels (Brown et al., 2008; Koga et al., 2011). In addition, although we checked all patients achieved the semantic tasks before investigations, neither behavioral performance nor response time was measured during ECoG recordings to avoid contamination of motor responses. Therefore, it was difficult to determine the HGA augmentation according to the response onset. Finally, the occipital pole or the medial surface of cortex was not sampled in the present study. Some ECoG studies previously showed the spatial–temporal characteristics of HGA augmentation involving these areas; thus these studies might supplement the weakness of this study (Brown et al., 2008; Wu et al., 2011).

We believe that our ECoG-normalization method is a novel and unique technique and can be used to provide information regarding human brain dynamics, which have been gradually unveiled by numerous previous language studies involving lesion-based and non-invasive imaging approaches.

Acknowledgements

References

Axmacher N, Mormann F, Fernandez G, Cohen MX, Elger CE, Fell J. Sustained neural activity patterns during working memory in the human medial temporal lobe. J Neurosci 2007;27:7807–16.

Baddeley A. Working memory. Science 1992;255:556–9.

Baddeley A, Hitch G. Working memory. In: Bower GH, editor. The psychology of learning and motivation. San Diego: Academic Press; 1974. p. 47–90.

Badre D, Wagner AD. Left ventrolateral prefrontal cortex and the cognitive control of memory. Neuropsychologia 2007;45:2883–901.

Benjamini Y, Hochberg Y. Controlling the false discovery rate – a practical and powerful approach to multiple testing. J Roy Statist Soc Ser B 1995;57:289–300.

Binder JR, Desai RH, Graves WW, Conant LL. Where is the semantic system? A critical review and meta-analysis of 120 functional neuroimaging studies. Cereb Cortex 2009;19:2767–96.

Binder JR, Frost JA, Hammeke TA, Bellgowan PS, Springer JA, Kaufman JN, et al. Human temporal lobe activation by speech and nonspeech sounds. Cereb Cortex 2000;10:512–28.

Binder JR, Medler DA, Westbury CF, Liebenthal E, Buchanan L. Tuning of the human left fusiform gyrus to sublexical orthographic structure. Neuroimage 2006;33:739–48.

Brown EC, Rothermel R, Nishida M, Juhasz C, Muzik O, Hoechstetter K, et al. In vivo animation of auditory-language-induced gamma-oscillations in children with intractable focal epilepsy. Neuroimage 2008;41:1120–31.

Buchsbaum BR, Hickok G, Humphries C. Role of left posterior superior temporal gyrus in phonological processing for speech perception and production. Cogn Sci 2001;25:663–78.

Canolty RT, Soltani M, Dalal SS, Edwards E, Dronkers NF, Nagarajan SS, et al. Spatiotemporal dynamics of word processing in the human brain. Front Neurosci 2007;1:185–96.

Champod AS, Petrides M. Dissociable roles of the posterior parietal and the prefrontal cortex in manipulation and monitoring processes. Proc Natl Acad Sci USA 2007;104:14837–42.

Champod AS, Petrides M. Dissociation within the frontoparietal network in verbal working memory: a parametric functional magnetic resonance imaging study. J Neurosci 2010;30:3849–56.

Cohen L, Lehericy S, Chochon F, Lemer C, Rivaud S, Dehaene S. Language-specific tuning of visual cortex? Functional properties of the Visual Word Form Area. Brain 2002;125:1054–69.

Crone NE, Boatman D, Gordon B, Hao L. Induced electrocorticographic gamma activity during auditory perception. Brazier Award-winning article. 2001. Clin Neurophysiol 2001a;112:565–82.

Crone NE, Hao L, Hart Jr J, Boatman D, Lesser RP, Irizarry R, et al. Electrocorticographic gamma activity during word production in spoken and sign language. Neurology 2001b;57:2045–53.

Crone NE, Miglioretti DL, Gordon B, Lesser RP. Functional mapping of human sensorimotor cortex with electrocorticographic spectral analysis. II. Event-related synchronization in the gamma band. Brain 1998;121(Pt 12):2301–15.

Curran T, Tucker DM, Kutas M, Posner MI. Topography of the N400: brain electrical activity reflecting semantic expectancy. Electroencephalogr Clin Neurophysiol 1993;88:188–209.

D'Ausilio A, Pulvermuller F, Salmas P, Bufalari I, Begliomini C, Fadiga L. The motor somatotopy of speech perception. Curr Biol 2009;19:381–5.

Dehaene S, Cohen L, Sigman M, Vinckier F. The neural code for written words: a proposal. Trends Cogn Sci 2005;9:335–41.

Dhond RP, Witzel T, Dale AM, Halgren E. Spatiotemporal cortical dynamics underlying abstract and concrete word reading. Hum Brain Mapp 2007;28:355–62.

Dronkers NF, Wilkins DP, Van Valin Jr RD, Redfern BB, Jaeger JJ. Lesion analysis of the brain areas involved in language comprehension. Cognition 2004;92:145–77.

Duffau H, Capelle L, Denvil D, Gatignol P, Sichez N, Lopes M, et al. The role of dominant premotor cortex in language: a study using intraoperative functional mapping in awake patients. Neuroimage 2003;20:1903–14.

Edwards E, Nagarajan SS, Dalal SS, Canolty RT, Kirsch HE, Barbaro NM, et al. Spatiotemporal imaging of cortical activation during verb generation and picture naming. Neuroimage 2010;50:291–301.

Edwards E, Soltani M, Deouell LY, Berger MS, Knight RT. High gamma activity in response to deviant auditory stimuli recorded directly from human cortex. J Neurophysiol 2005;94:4269–80.

Fiez JA. Phonology, semantics, and the role of the left inferior prefrontal cortex. Hum Brain Mapp 1997;5:79–83.

Friederici AD, Ruschemeyer SA, Hahne A, Fiebach CJ. The role of left inferior frontal and superior temporal cortex in sentence comprehension: localizing syntactic and semantic processes. Cereb Cortex 2003;13:170–7.

Genovese CR, Lazar NA, Nichols T. Thresholding of statistical maps in functional neuroimaging using the false discovery rate. Neuroimage 2002;15:870–8.

Halgren E, Dhond RP, Christensen N, Van Petten C, Marinkovic K, Lewine JD, et al. N400-like magnetoencephalography responses modulated by semantic context, word frequency, and lexical class in sentences. Neuroimage 2002;17:1101–16.

Hashimoto R, Sakai KL. Specialization in the left prefrontal cortex for sentence comprehension. Neuron 2002;35:589–97.

Helenius P, Salmelin R, Service E, Connolly JF. Distinct time courses of word and context comprehension in the left temporal cortex. Brain 1998;121(Pt 6):1133–42.

Herholz, K., Reulen, H.J., von Stockhausen, H.M., Thiel, A., Ilmberger, J., Kessler, J., et al. Preoperative activation and intraoperative stimulation of language-related areas in patients with glioma. Neurosurgery 1997; 41: 1253–1260; discussion 1260–1252.

Hickok G. Functional anatomy of speech perception and speech production: psycholinguistic implications. J Psycholinguist Res 2001;30:225–35.

Hickok G, Buchsbaum B, Humphries C, Muftuler T. Auditory-motor interaction revealed by fMRI: speech, music, and working memory in area Spt. J Cogn Neurosci 2003;15:673–82.

Hickok G, Poeppel D. Dorsal and ventral streams: a framework for understanding aspects of the functional anatomy of language. Cognition 2004;92:67–99.

Hickok G, Poeppel D. The cortical organization of speech processing. Nat Rev Neurosci 2007;8:393–402.

Homae F, Hashimoto R, Nakajima K, Miyashita Y, Sakai KL. From perception to sentence comprehension: the convergence of auditory and visual information of language in the left inferior frontal cortex. Neuroimage 2002;16:883–900.

Homae F, Yahata N, Sakai KL. Selective enhancement of functional connectivity in the left prefrontal cortex during sentence processing. Neuroimage 2003;20:578–86.

Howard MW, Rizzuto DS, Caplan JB, Madsen JR, Lisman J, Aschenbrenner-Scheibe R, et al. Gamma oscillations correlate with working memory load in humans. Cereb Cortex 2003;13:1369–74.

Humphries C, Willard K, Buchsbaum B, Hickok G. Role of anterior temporal cortex in auditory sentence comprehension: an fMRI study. Neuroreport 2001;12:1749–52.

Johnson BW, Hamm JP. High-density mapping in an N400 paradigm: evidence for bilateral temporal lobe generators. Clin Neurophysiol 2000;111:532–45.

Jonides J, Schumacher EH, Smith EE, Koeppe RA, Awh E, Reuter-Lorenz PA, et al. The role of parietal cortex in verbal working memory. J Neurosci 1998;18:5026–34.

Jung J, Mainy N, Kahane P, Minotti L, Hoffmann D, Bertrand O, et al. The neural bases of attentive reading. Hum Brain Mapp 2008;29:1193–206.

Kamada K, Sawamura Y, Takeuchi F, Kuriki S, Kawai K, Morita A, et al. Expressive and receptive language areas determined by a non-invasive reliable method using functional magnetic resonance imaging and magnetoencephalography. Neurosurgery 2007;60:296–305.

Koga S, Rothermel R, Juhasz C, Nagasawa T, Sood S, Asano E. Electrocorticographic correlates of cognitive control in a Stroop task-intracranial recording in epileptic patients. Hum Brain Mapp 2011;32:1580–91.

Kunii, N., Kamada, K., Ota, T., Kawai, K., Saito, N. A detailed analysis of functional magnetic resonance imaging in the frontal language area – a comparative study with extraoperative electrocortical stimulation. Neurosurgery 2011; 69: 590–596; discussion 596–597.

Lachaux JP, George N, Tallon-Baudry C, Martinerie J, Hugueville L, Minotti L, et al. The many faces of the gamma band response to complex visual stimuli. Neuroimage 2005;25:491–501.

Laviolette PS, Rand SD, Ellingson BM, Raghavan M, Lew SM, Schmainda KM, et al. 3D visualization of subdural electrode shift as measured at craniotomy reopening. Epilepsy Res 2011;94:102–9.

Leuthardt, E.C., Miller, K., Anderson, N.R., Schalk, G., Dowling, J., Miller, J., et al. Electrocorticographic frequency alteration mapping: a clinical technique for mapping the motor cortex. Neurosurgery 2007; 60: 260–270; discussion 270–261.

MacDonald III AW, Cohen JD, Stenger VA, Carter CS. Dissociating the role of the dorsolateral prefrontal and anterior cingulate cortex in cognitive control. Science 2000;288:1835–8.

Maess B, Herrmann CS, Hahne A, Nakamura A, Friederici AD. Localizing the distributed language network responsible for the N400 measured by MEG during auditory sentence processing. Brain Res 2006;1096:163–72.

Mainy N, Jung J, Baciu M, Kahane P, Schoendorff B, Minotti L, et al. Cortical dynamics of word recognition. Hum Brain Mapp 2008;29:1215–30.

Makeig S. Auditory event-related dynamics of the EEG spectrum and effects of exposure to tones. Electroencephalogr Clin Neurophysiol 1993;86:283–93.

Martin A, Haxby JV, Lalonde FM, Wiggs CL, Ungerleider LG. Discrete cortical regions associated with knowledge of color and knowledge of action. Science 1995;270:102–5.

Martin A, Wiggs CL, Ungerleider LG, Haxby JV. Neural correlates of category-specific knowledge. Nature 1996;379:649–52.

Meltzer JA, Zaveri HP, Goncharova II, Distasio MM, Papademetris X, Spencer SS, et al. Effects of working memory load on oscillatory power in human intracranial EEG. Cereb Cortex 2008;18:1843–55.

Miller KJ, Leuthardt EC, Schalk G, Rao RP, Anderson NR, Moran DW, et al. Spectral changes in cortical surface potentials during motor movement. J Neurosci 2007;27:2424–32.

Moore CJ, Price CJ. A functional neuroimaging study of the variables that generate category-specific object processing differences. Brain 1999;122(Pt 5):943–62.

Nagasawa T, Matsuzaki N, Juhasz C, Hanazawa A, Shah A, Mittal S, et al. Occipital gamma-oscillations modulated during eye movement tasks: simultaneous eye tracking and electrocorticography recording in epileptic patients. Neuroimage 2011;58:1101–9.

Newman SD, Just MA, Keller TA, Roth J, Carpenter PA. Differential effects of syntactic and semantic processing on the subregions of Broca's area. Brain Res Cogn Brain Res 2003;16:297–307.

Ni W, Constable RT, Mencl WE, Pugh KR, Fulbright RK, Shaywitz SE, et al. An event-related neuroimaging study distinguishing form and content in sentence processing. J Cogn Neurosci 2000;12:120–33.

Noppeney U, Josephs O, Kiebel S, Friston KJ, Price CJ. Action selectivity in parietal and temporal cortex. Brain Res Cogn Brain Res 2005;25:641–9.

Noppeney U, Phillips J, Price C. The neural areas that control the retrieval and selection of semantics. Neuropsychologia 2004;42:1269–80.

Ojemann G, Ojemann J, Lettich E, Berger M. Cortical language localization in left, dominant hemisphere. An electrical stimulation mapping investigation in 117 patients. J Neurosurg 1989;71:316–26.

Ossadtchi A, Greenblatt RE, Towle VL, Kohrman MH, Kamada K. Inferring spatiotemporal network patterns from intracranial EEG data. Clin Neurophysiol 2010;121:823–35.

Pei X, Leuthardt EC, Gaona CM, Brunner P, Wolpaw JR, Schalk G. Spatiotemporal dynamics of electrocorticographic high gamma activity during overt and covert word repetition. Neuroimage 2011;54:2960–72.

Penfield W, Roberts L. Speech and brain-mechanisms. Princeton, NJ: Princeton University Press; 1959.

Pfurtscheller G, Lopes da Silva FH. Event-related EEG/MEG synchronization and desynchronization: basic principles. Clin Neurophysiol 1999;110:1842–57.

Polk TA, Drake RM, Jonides JJ, Smith MR, Smith EE. Attention enhances the neural processing of relevant features and suppresses the processing of irrelevant features in humans: a functional magnetic resonance imaging study of the Stroop task. J Neurosci 2008;28:13786–92.

Price CJ. The anatomy of language: a review of 100 fMRI studies published in 2009. Ann NY Acad Sci 2010;1191:62–88.

Pulvermuller F, Huss M, Kherif F, Moscoso del Prado Martin F, Hauk O, Shtyrov Y. Motor cortex maps articulatory features of speech sounds. Proc Natl Acad Sci USA 2006;103:7865–70.

Pylkkanen L, McElree B. An MEG study of silent meaning. J Cogn Neurosci 2007;19:1905–21.

Rauschecker JP. Cortical processing of complex sounds. Curr Opin Neurobiol 1998;8:516–21.

Ravizza SM, Delgado MR, Chein JM, Becker JT, Fiez JA. Functional dissociations within the inferior parietal cortex in verbal working memory. Neuroimage 2004;22:562–73.

Ray S, Niebur E, Hsiao SS, Sinai A, Crone NE. High-frequency gamma activity (80–150 Hz) is increased in human cortex during selective attention. Clin Neurophysiol 2008;119:116–33.

Salmelin R, Hari R, Lounasmaa OV, Sams M. Dynamics of brain activation during picture naming. Nature 1994;368:463–5.

Scott SK, Blank CC, Rosen S, Wise RJ. Identification of a pathway for intelligible speech in the left temporal lobe. Brain 2000;123(Pt 12):2400–6.

Sederberg PB, Schulze-Bonhage A, Madsen JR, Bromfield EB, McCarthy DC, Brandt A, et al. Hippocampal and neocortical gamma oscillations predict memory formation in humans. Cereb Cortex 2007;17:1190–6.

Sinai A, Bowers CW, Crainiceanu CM, Boatman D, Gordon B, Lesser RP, et al. Electrocorticographic high gamma activity versus electrical cortical stimulation mapping of naming. Brain 2005;128:1556–70.

Sinai A, Crone NE, Wied HM, Franaszczuk PJ, Miglioretti D, Boatman-Reich D. Intracranial mapping of auditory perception: event-related responses and electrocortical stimulation. Clin Neurophysiol 2009;120:140–9.

Tallon-Baudry C, Bertrand O, Henaff MA, Isnard J, Fischer C. Attention modulates gamma-band oscillations differently in the human lateral occipital cortex and fusiform gyrus. Cereb Cortex 2005;15:654–62.

Tanji K, Suzuki K, Delorme A, Shamoto H, Nakasato N. High-frequency gamma-band activity in the basal temporal cortex during picture-naming and lexical-decision tasks. J Neurosci 2005;25:3287–93.

Thompson-Schill SL, D'Esposito M, Aguirre GK, Farah MJ. Role of left inferior prefrontal cortex in retrieval of semantic knowledge: a reevaluation. Proc Natl Acad Sci USA 1997;94:14792–7.

Thompson-Schill SL, D'Esposito M, Kan IP. Effects of repetition and competition on activity in left prefrontal cortex during word generation. Neuron 1999;23:513–22.

Thompson-Schill SL, Swick D, Farah MJ, D'Esposito M, Kan IP, Knight RT. Verb generation in patients with focal frontal lesions: a neuropsychological test of neuroimaging findings. Proc Natl Acad Sci USA 1998;95:15855–60.

Trautner P, Rosburg T, Dietl T, Fell J, Korzyukov OA, Kurthen M, et al. Sensory gating of auditory evoked and induced gamma band activity in intracranial recordings. Neuroimage 2006;32:790–8.

Tsapkini K, Rapp B. The orthography-specific functions of the left fusiform gyrus: evidence of modality and category specificity. Cortex 2010;46:185–205.

Tse CY, Lee CL, Sullivan J, Garnsey SM, Dell GS, Fabiani M, et al. Imaging cortical dynamics of language processing with the event-related optical signal. Proc Natl Acad Sci USA 2007;104:17157–62.

Tsukiura T, Fujii T, Takahashi T, Xiao R, Inase M, Iijima T, et al. Neuroanatomical discrimination between manipulating and maintaining processes involved in verbal working memory: a functional MRI study. Brain Res Cogn Brain Res 2001;11:13–21.

Uusvuori J, Parviainen T, Inkinen M, Salmelin R. Spatiotemporal interaction between sound form and meaning during spoken word perception. Cereb Cortex 2008;18:456–66.

van Vugt MK, Schulze-Bonhage A, Litt B, Brandt A, Kahana MJ. Hippocampal gamma oscillations increase with memory load. J Neurosci 2010;30:2694–9.

Vartiainen J, Parviainen T, Salmelin R. Spatiotemporal convergence of semantic processing in reading and speech perception. J Neurosci 2009;29:9271–80.

Vigneau M, Beaucousin V, Herve PY, Duffau H, Crivello F, Houde O, et al. Meta-analyzing left hemisphere language areas: phonology, semantics, and sentence processing. Neuroimage 2006;30:1414–32.

Wagner AD, Pare-Blagoev EJ, Clark J, Poldrack RA. Recovering meaning: left prefrontal cortex guides controlled semantic retrieval. Neuron 2001;31:329–38.

Wilson SM, Saygin AP, Sereno MI, Iacoboni M. Listening to speech activates motor areas involved in speech production. Nat Neurosci 2004;7:701–2.

Wu HC, Nagasawa T, Brown EC, Juhasz C, Rothermel R, Hoechstetter K, et al. Gamma-oscillations modulated by picture naming and word reading: intracranial recording in epileptic patients. Clin Neurophysiol 2011;122:1929–42.

Wu M, Wisneski K, Schalk G, Sharma M, Roland J, Breshears J, et al. Electrocorticographic frequency alteration mapping for extraoperative localization of speech cortex. Neurosurgery 2010;66:E407–9.

Yuval-Greenberg S, Tomer O, Keren AS, Nelken I, Deouell LY. Transient induced gamma-band response in EEG as a manifestation of miniature saccades. Neuron 2008;58:429–41.

Zygierewicz J, Durka PJ, Klekowicz H, Franaszczuk PJ, Crone NE. Computationally efficient approaches to calculating significant ERD/ERS changes in the time-frequency plane. J Neurosci Methods 2005;145:267–76.

てんかんに対する迷走神経刺激療法の実施ガイドライン

川合謙介*
日本てんかん学会ガイドライン作成委員会
委員長　須貝研司
委　員　赤松直樹、岡崎光俊、亀山茂樹、笹川睦男、辻　貞俊、前原健寿、山本　仁
＊東京大学大学院医学系研究科

1.　はじめに

　迷走神経刺激療法 vagus nerve stimulation（VNS）は、てんかんに対する非薬剤治療のひとつであり、抗てんかん薬に抵抗する難治性てんかん発作を減少、軽減する緩和的治療である。植込型の電気刺激装置により、左頸部迷走神経を間歇的に刺激する。欧米では1990年代から行われており、わが国でも2010年7月から保険適用となった。

　VNS は本邦初のてんかんに対する植込型装置による電気刺激療法であり、治療適応や施行方法についての混乱を避けるため、日本てんかん学会としてのガイドラインを提示する。

2.　VNS の目的

Q.　VNS は効果があるか？

> VNS は薬剤抵抗性てんかん発作に対して緩和効果がある。【推奨度 A】

解説

　VNS の治療対象は薬剤抵抗性のてんかん発作であり、てんかん発作の緩和を目的に施行する[1,2]。VNS はあくまで緩和的治療であり、発作の完全消失を目指すものではない。てんかん発作の緩和効果の他に、てんかん患者にみられる認知機能障害・情動障害などの随伴症状に対する有効性が報告されているが[3-5]、これらはてんかん発作に対して施行された VNS を利用した研究であり、随伴症状に対する効果を主目的とした study design としては十分なものではない。したがって、随伴症状の軽減を主目的とする治療適応を支持する十分な科学的根拠とはならない。

3.　VNS の対象患者

Q.　VNS はどのような患者とてんかん発作が対象となるか？

> 薬剤抵抗性のてんかん発作で開頭手術の対象とならない発作【推奨度 C】

解説

　VNS の有効性は、米国で行われた12歳以上の部分発作を対象とする二つの無作為対照試験で検証された[1,2]。これらの試験では、治療3ヶ月での強刺激群と弱刺激群における平均発作減少率は各々25-28%、6-15% であった。

　一方、小児や全般発作に対する無作為対照試験は行われていない。しかし、多くの症例シリーズ研究で有効性が報告されている[6-8]。したがって、小児や全般発作に対して使用する場合は慎重に適応を判断し、治療開始後も有効性と有害事象に関する追跡調査を行う必要がある。本邦では薬事承認の際に厚生労働省から、12歳未満の小児全例での使用成績調査が義務付けられた。